

Discovery and Mechanistic Study of Tailor-Made Quinoline Derivatives as Topoisomerase 1 Poison with Potent Anticancer Activity

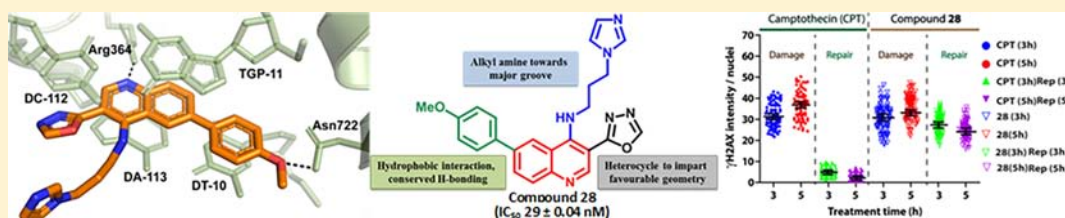
Biswajit Kundu,^{†,||} Subhendu K. Das,^{‡,||} Srijita Paul Chowdhuri,^{‡,||} Sourav Pal,^{†,§} Dipayan Sarkar,^{†,§} Arijit Ghosh,[‡] Ayan Mukherjee,^{†,§} Debomita Bhattacharya,[†] Benu Brata Das,^{*,‡,§} and Arindam Talukdar^{*,†,||}

[†]Department of Organic and Medicinal Chemistry, CSIR-Indian Institute of Chemical Biology, 4 Raja S. C. Mullick Road, Kolkata 700032, West Bengal, India

[‡]Laboratory of Molecular Biology, School of Biological Sciences; Indian Association for the Cultivation of Science, 2A & 2B, Raja S. C. Mullick Road, Kolkata, 700032 West Bengal, India

[§]Academy of Scientific and Innovative Research, Kolkata 700032, West Bengal, India

S Supporting Information



ABSTRACT: To overcome chemical limitations of camptothecin (CPT), we report design, synthesis, and validation of a quinoline-based novel class of topoisomerase 1 (Top1) inhibitors and establish that compound 28 (*N*-(3-(1*H*-imidazol-1-yl)propyl)-6-(4-methoxyphenyl)-3-(1,3,4-oxadiazol-2-yl)quinolin-4-amine) exhibits the highest potency in inhibiting human Top1 activity with an IC_{50} value of 29 ± 0.04 nM. Compound 28 traps Top1–DNA cleavage complexes (Top1ccs) both in the *in vitro* cleavage assays and in live cells. Point mutation of Top1-N722S fails to trap compound 28-induced Top1cc because of its inability to form a hydrogen bond with compound 28. Unlike CPT, compound 28 shows excellent plasma serum stability and is not a substrate of P-glycoprotein 1 (permeability glycoprotein) advancing its potential anticancer activity. Finally, we provide evidence that compound 28 overcomes the chemical instability of CPT in human breast adenocarcinoma cells through generation of persistent and less reversible Top1cc-induced DNA double-strand breaks as detected by γ H2AX foci immunostaining after 5 h of drug removal.

INTRODUCTION

Topoisomerases are ubiquitous enzymes, which are indispensable for relaxing the topological constraints arising during the DNA metabolic processes of replication, transcription, and chromatin remodeling.^{1–4} Human topoisomerase 1 (HTop1) creates a single-stranded nick onto the DNA by a nucleophilic attack on the DNA phosphodiester bond to form a “cleavage complex” in which the enzyme is covalently linked to the 3′ end of the broken DNA strand (Top1–DNA cleavage complexes, Top1ccs). This is then followed by a “controlled rotation” of the broken scissile strand around the intact strand, resulting in the relaxation of the DNA superhelical tension. Eventually, the 5′ end of the scissile strand mediates a nucleophilic attack on the phosphotyrosyl–DNA phosphodiester to religate the DNA and release the enzyme, which ends the catalytic cycle of the enzyme.^{5,6} Trapped Top1ccs generate detrimental lesions, which lead to the formation of DNA double-strand breaks (DSBs) upon collision with ongoing replication forks and/or transcription machinery and are

accountable for the killing of proliferating malignant cancer cells.^{2,7–9}

There are two types of topoisomerase inhibitors, which include catalytic inhibitors and poisons.^{2,5,10,11} Catalytic inhibitors directly bind with the free topoisomerase and inhibit its catalytic activity.^{12,13} While poisons reveal their anticancer activity by selectively trapping the Top1–DNA covalent cleavage complexes^{9,14,15} inside cells, which include camptothecin (CPT)¹⁶ and its clinical derivatives as well as several non-CPT Top1 poisons including indenoisoquinolines,^{17,18} indolocarbazoles,¹⁹ and thiohydantoin²⁰ derivatives. Clinical derivatives of CPT such as topotecan and irinotecan are used for advanced colorectal carcinomas and ovarian cancers. However, CPT and its derivatives suffer from dose-limiting toxicity, resulting in severe diarrhea and neutropenia, rapidly inactivated in plasma because of hydrolysis of lactone E-ring

Received: December 11, 2018

Published: March 21, 2019

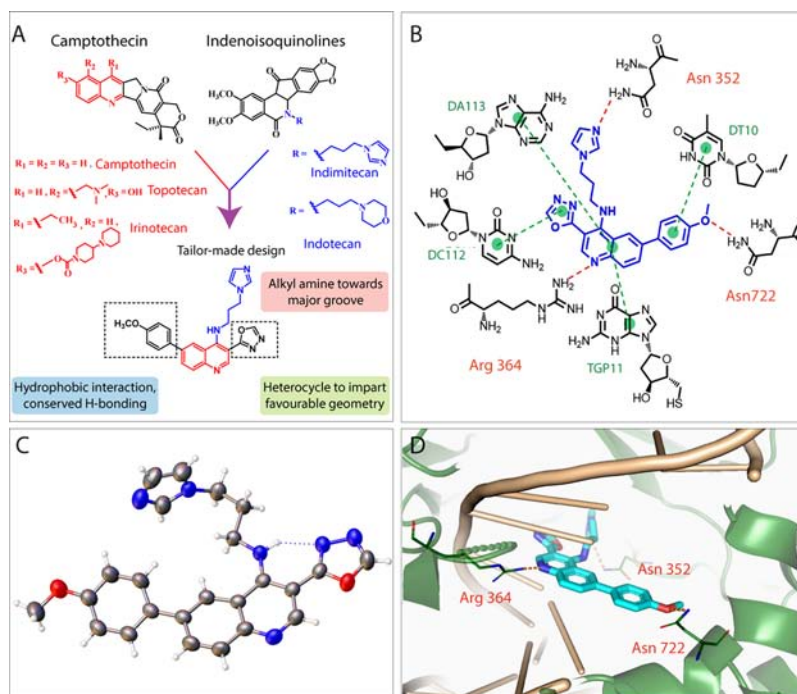


Figure 1. (A) Design of tailor-made analogue conceived from the structural features of known ligand and analysis of the active site; (B) 2D binding interactions of compound **28** with the important amino acid residues and base pairs. Red dotted lines indicate hydrogen bond and green dotted lines indicate π - π stacking interaction; (C) X-ray crystal structure of compound **28**; (D) hypothetical binding model of the ternary complex of human Top1-DNA-**28**. The structure was generated from the crystal structure of Top1-DNA-CPT (PDB ID: 1T8I).

and binding of the ensuing hydroxyl acid to plasma proteins, and finally accumulate resistance in the topoisomerase 1 (Top1) gene.^{6,15} CPT was also found to be a substrate of permeability glycoprotein (Pgp).²¹ Moreover, irinotecan is a prodrug, which requires a carboxylesterase enzyme to convert into an active metabolite.²² Recent advances in developing a non-CPT Top1-targeted drug lead to the discovery of indenoisoquinolines (indotecan and indimitecan), which are in clinical trials for treatment in adults with solid tumors and lymphomas.^{15,22,23}

Here, we report the design, synthesis, mechanism study, and validation of a novel class of Top1 poisons based on the quinoline core, identified through the structural features of known ligands (CPT, topotecan, irinotecan, and indenoisoquinolines) that bind through the network of interactions in the active site of human Top1 enzyme as revealed by cocrystal structures^{18,24–29} (Figure 1A) for potent anticancer activity. Compound **28**-mediated induction of Top1cc formation in live cells was substantiated by fluorescence recovery after photobleaching (FRAP) assays. We also show that Top1-N722^{30,31} is critical for the compound's in vivo trapping of Top1cc in cancer cells treated with compound **28**. We provide compelling in vitro absorption, distribution, metabolism, and excretion (ADME), biochemical, and cellular evidence that advocate compound **28** as a potential anticancer agent.

CHEMISTRY

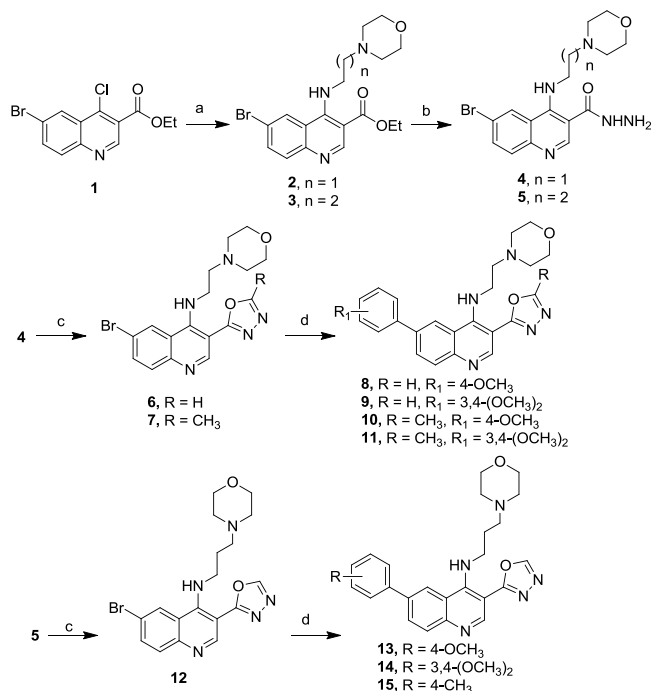
Compound **1** was treated with suitable aminoalkyl amines in the presence of a base [*N,N*-diisopropylethylamine (DIPEA)] in 1,4-dioxane solvent to afford compounds **2** and **3** in excellent yield. Compound **2** or **3** was dissolved in ethanol and treated with the solution of hydrazine monohydrate to obtain compounds **4** and **5**. Compound **6** was prepared by heating compound **4** with triethyl orthoformate at 110 °C for 12 h.

Similarly, compound **4** was refluxed with triethyl orthoacetate in ethanol for 8 h to obtain **7**. Compound **4** was subjected to Suzuki coupling reaction with suitable boronic acids to get compounds **8–11**. A similar Suzuki reaction of **5** with the respective boronic acid provided compounds **13–15** (Scheme 1). By following the similar reaction sequence (Scheme 2), imidazole analogues were produced. Finally, the Suzuki coupling reaction was performed to produce a series of compounds (**22–34**).

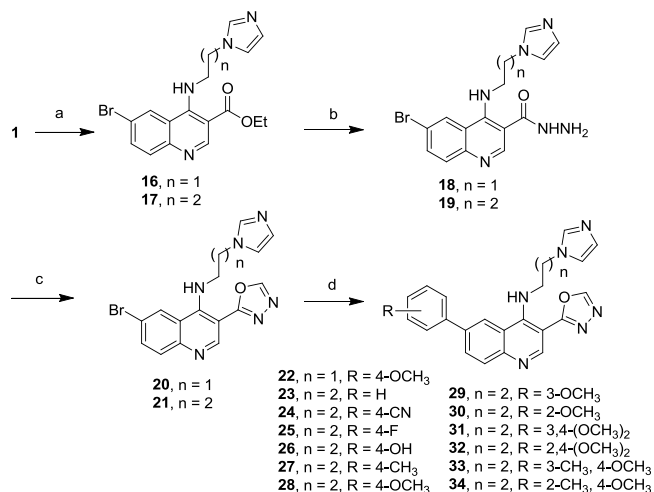
In Scheme 3, compound **19** was converted to oxadiazol-2-amine derivative **35** and oxadiazol-5-methyl derivative **37** by treating with cyanogen bromide in methanol and triethyl orthoacetate in ethanol, respectively, under refluxing condition. Suzuki reaction of **35** and **37** with 2-(4-methoxyphenyl)-boronic ester provided compounds **36** and **38**, respectively. Similar Suzuki reaction of **17** with the respective boronic acid provided compounds **39** and **40**. By following the similar reaction sequence in Scheme 1, compound **1** was converted to methylamine derivative **41**, followed by hydrazine derivative **42**. Subsequent oxadiazole formation with triethyl orthoformate leads to compound **43**, which on Suzuki coupling with 2-(4-methoxyphenyl)boronic ester provided compound **44**. All compounds subjected to assay were checked for >95% purity by high-performance liquid chromatography (HPLC).

RESULTS AND DISCUSSION

Design of the Top1 Inhibitor. The basis of design has been depicted in Figure 1A or 1B. As CPT and its clinically approved derivatives topotecan and irinotecan suffer from several limitations, we embarked on the discovery of “non-CPT” Top1 poisons^{21,32} with improved efficacy. We initiated our design from the quinoline core, which is also shared by CPT and its clinically approved derivatives topotecan and irinotecan (Figure 1A). The substitution pattern on the

Scheme 1^a

^aReagents and conditions: (a) 2-morpholinoethanamine (for 2) or 3-morpholinopropan-1-amine (for 3), DIPEA, 1,4-dioxane, rt, 12 h; (b) hydrazine monohydrate, EtOH, rt, 8–12 h; (c) triethyl orthoformate, 110 °C, 12 h (for 6 and 12) or triethyl orthoacetate, EtOH, reflux, 8 h (for 7); (d) 2-(4-methoxyphenyl)-4,4,5,5-tetramethyl-1,3,2-dioxaborolane (for 8, 10, and 13), (3,4-dimethoxyphenyl)boronic acid (for 9, 11, and 14), *p*-tolylboronic acid (for 15), Pd(PPh₃)₄, 2 M Na₂CO₃, 1,4-dioxane, 100 °C, 8–12 h.

Scheme 2^a

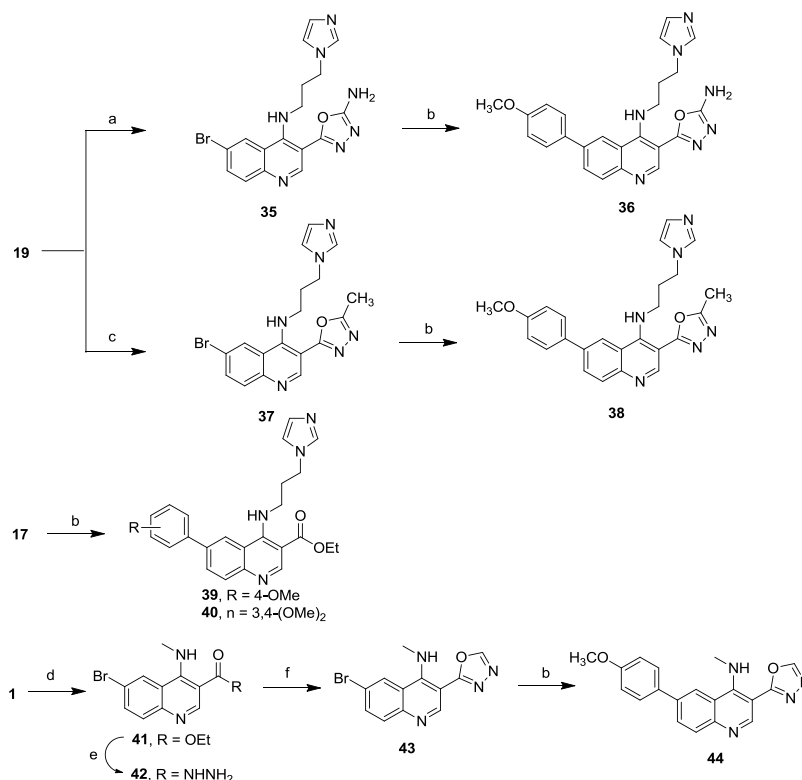
^aReagents and conditions: (a) 2-(1*H*-imidazole-1-yl)ethanamine (for 16) or 1-(3-aminopropyl)imidazole (for compound 17), DIPEA, 1,4-dioxane, rt (for 17) or 100 °C (for 16), 12 h; (b) hydrazine monohydrate, EtOH, rt, 8–12 h; (c) triethyl orthoformate, 100 °C, 12 h; (d) various boronic acids, Pd(PPh₃)₄, 2 M Na₂CO₃, 1,4-dioxane, 100 °C, 7–24 h.

quinoline core was strategically positioned at C-3, C-4, and C-6 to avail the conserved hydrogen bond interactions and hydrophobic interactions such as π – π stacking and to attain the requisite geometry to be able to stabilize the Top1–DNA

cleavage complex (Figure 1B).⁵ In the indenoisoquinoline series, the importance of a suitable alkyl amino chain containing a heteroatom has been previously validated as it is capable of serving as a hydrogen-bond acceptor into the major groove of the ternary complex.^{33–35} Also, the dimethylamine group in topotecan is predicted to project into the major groove to attain similar interactions. We presumed that similar alkyl amino chain at the C-4 position of the quinoline core will project in the major groove toward interacting residue Asn352. The alkyl chain-attached heterocycle installed at C-4 can serve a similar purpose and attain similar interactions as observed in indenoisoquinoline and CPT derivatives.³⁶ The crystal structures of the ternary complex of CPT and indenoisoquinoline revealed the importance of polycyclic rings with flat planar geometry that can accommodate in the interface of the Top1–DNA cleavage complexes and block the religation reaction. We envisioned that the strategically placed C-6-substituted aromatic ring along with a heterocycle at the C-3 position would impart requisite geometry and suitable curvature essential to attain the conserved hydrogen bond interactions as well as hydrophobic interactions such as π – π stacking for stabilizing the Top1–DNA cleavage complex (Figure 1B). As a next logical step, we explored the nature of substitution on the aromatic ring at C-6 and on heterocycles at C-3 that can modulate Top1 inhibition to identify potent Top1 poison.

Related to Top1 inhibition, half-maximal inhibitory concentration (IC₅₀) values for the designed analogues were investigated in plasmid DNA relaxation inhibition assays by using either recombinant Top1 or MCF7 cellular lysates as a source of Top1 (Table 1). We used both biochemical and cellular studies to validate the mechanism of Top1 inhibition. Further insight into the ability of the potent Top1 inhibitor (compound 28) to trap mutant Top1 at residue Asn722 was justified by FRAP assays in live cells. The accumulation and disappearance of DNA damage by the identified compounds were measured by immunological staining with phosphorylated histone H2AX (γ H2AX) under confocal microscopy. Subsequently, *in vitro* ADME studies were conducted to determine the metabolic stability and efflux property of these analogues.

Morpholine Analogues. We synthesized the first batch of compounds by keeping the alkyl-substituted morpholine group at the C-4 position, 4-methoxy and 3,4-dimethoxy phenyl groups at the C-6 position, and the oxadiazole group at C-3 (Scheme 1). The choice of substitution pattern at C-4 and C-6 positions was inspired from the structural features present in CPT derivatives and indenoisoquinoline derivatives (indotecan and indimitecan) (Figure 1A) established as Top1 poison, which are currently under clinical trials.^{15,23,34,37} Previous reports have suggested that installation of such moiety resulted in improved Top1 inhibitory activity.^{33,34} Compound 8 with two carbon morpholine groups at C-4 and the 4-methoxy group at C-6 and compound 9 with two carbon morpholine groups at C-4 and the 3,4-dimethoxy phenyl group at C-6 did not show significant Top1 inhibitory activity in the plasmid DNA relaxation assays at 10 μ M concentration (Table 1). Although 4-methoxy derivative 8 and 3,4-dimethoxy phenyl derivative 9 did not show significant inhibition at 10 μ M, at higher concentration (100 μ M) compound 8 showed 50% inhibition as compared to 9 with 20% inhibition. Installation of a methyl group at the C-5" position of the oxadiazole ring in 8 and 9 resulted in compounds 10 and 11 (Scheme 1), respectively, which also failed to show 50% Top1 inhibition

Scheme 3^a

^aReagents and conditions: (a) cyanogen bromide, MeOH, reflux, 4 h; (b) 2-(4-methoxyphenyl)-4,4,5,5-tetramethyl-1,3,2-dioxaborolane (for 36, 38, 39, and 44) or (3,4-dimethoxyphenyl)boronic acid (for 40), Pd(PPh₃)₄, 2 M Na₂CO₃, 1,4-dioxane, 100 °C, 6–12 h. (c) Triethyl orthoacetate, EtOH, reflux, 6 h; (d) methylamine, DIPEA, THF, 60 °C, 16 h; (e) hydrazine monohydrate, EtOH, rt, 12 h; (f) triethyl orthoformate, 140 °C, 14 h.

(Table 1) at 10 μ M concentration. Thereafter, we increased the chain length connected to the morpholine group at C-4 from two carbons to three carbons. Indeed, increasing the chain length in compound 13 with the 4-methoxyphenyl group at C-6 showed marked increase in Top1 inhibitory activity with an IC₅₀ value of 1.79 μ M against recombinant human Top1.^{20,38–40} However, 14 with the 3,4-dimethoxy phenyl group failed to inhibit at least 50% Top1 relaxation activity (Table 1) at 10 μ M concentration. An initial comparison between 8, 9, 13, and 14 suggests that combination of three carbon-chain lengths at C-4 with the monosubstitution of the 4-methoxyphenyl group at C-6 reinforces Top1 inhibitory activity. The importance of the 4-methoxyphenyl group at C-6 was further substantiated by replacement of the –OCH₃ group present at the C-6-substituted phenyl ring by a methyl group (–CH₃) in compound 15, leading to loss of activity. Taken together, the initial studies indicate that morpholine-substituted propylamine at C-4 and the 4-methoxyphenyl group at the C-6 position are two important features that can trigger Top1 inhibition in the quinoline core.

Imidazole Analogues. As both morpholine and imidazole groups are present in indotecan, indimitecan, and indenoisoquinolines derivatives, we replaced the C-4 substituents containing a morpholine moiety with imidazole in our newly synthesized analogues and investigated the Top1 inhibition. A series of compounds were prepared bearing an imidazole group with varying chain length at C-4, substituted phenyl group at C-6, and oxadiazole ring at C-3 (Scheme 2). On the basis of our previous observation which showed the importance of

morpholine-substituted propylamine at C-4, it seemed prudent to keep the chain length of the flexible aminoalkyl group to three carbon linkers. A series of compounds were prepared by substituting the C-4' position of the phenyl group at C-6 with cyano (24), fluoro (25), hydroxyl (26), methyl (27), and methoxy (28) group (Scheme 2). Compounds with cyano (24), fluoro (25), and hydroxyl (26) modifications failed to show significant Top1 inhibitory activity in plasmid DNA relaxation assays at 10 μ M (Table 1). Remarkably, compound 28 bearing a 4-methoxy group at C-4' showed the highest ability to inhibit recombinant Top1 activity with an IC₅₀ of 29 nM in the plasmid DNA relaxation assay (Table 1).¹² Notably, compound 27 with 4-methyl substitution at the C-4' position of the phenyl group also showed Top1 inhibitory activity with an IC₅₀ value of 1.06 μ M in Top1 inhibition. Installing the unsubstituted phenyl group at C-6 in 23 resulted in a sharp decrease in Top1 inhibitory activity (40% inhibition at 10 μ M). A direct comparison of the activities of morpholine (13 and 15) and imidazole series (23 and 27) shows that the imidazole-substituted propylamine at C-4 along with the 4-methoxyphenyl group at the C-6 position confers increased Top1 inhibitory activity.

For a better understanding, hypothetical binding model of 28–Top1–DNA ternary complex was constructed with the human Top1 crystal structure (PDB code 1T8I). The oxygen atom of the methoxy group forms a hydrogen bonding interaction with Asn722 in the C-terminal domain of Top1. Asn722 is an important amino acid responsible for binding of the ligands with Top1 cleavage complexes.⁴¹ The nitrogen

Table 1. Analysis of Human Top1 Inhibition in Plasmid DNA Relaxation Assays with Recombinant Top1 (In vitro) or MCF7 Cell Lysates (Ex vivo)

Comp	R ₁	R ₂	R ₃	Top1 inhibition IC ₅₀ (μM)		Activity index ^a
				<i>In vitro</i>	<i>Ex vivo</i>	
CPT				0.025	2.5	++++
Topotecan				0.021	1.8	++++
8				>10	NT ^b	+
9				>10	NT	+
10				>10	NT	+
11				>10	NT	+
13				1.79 ± 0.62	2.51 ± 0.39	+++
14				>10	NT	+
15				>10	NT	+
22				>10	NT	+
23				>10	NT	+
24				>10	NT	+
25				>10	NT	+
26				>10	NT	+
27				1.06±0.417	3.75±0.102	+++
28				0.029±0.004	2.74±0.314	++++
29				1.054±0.792	4.11±0.339	+++
30				>10	NT	+
31				>10	NT	+
32				>10	NT	+
33				2.36±0.884	3±0.98	++
34				>10	NT	+
36				>10	NT	+
38				>10	NT	+
39				>10	NT	+
40				>10	NT	+
44				>10	NT	+

^aCompound-induced in vitro inhibition of Top1 with scores given according to the following system based on the activity of CPT: + = IC₅₀ > 10 μM; ++ = IC₅₀ in between 2 and 10 μM; +++ = IC₅₀ in between 100 nM and 2 μM; ++++ = IC₅₀ < 100 nM. ^bNT = Not tested.

atom in the quinoline ring also forms a hydrogen bond with Arg364, and the three carbon alkyl chain length is ideal for the imidazole ring to attain hydrogen bond interaction with Asn352. The aminopropylamino chain at C-4 and the 4-methoxyphenyl group substitution at the C-6 position of the quinoline ring come in contact with Top1cc and DNA, which may be attributed to Top1 inhibition (Figure 1B,D). In keeping with the docking analysis (Figure 1B,D), the X-ray

crystal structure of compound 28 (Figure 1C) reveals that it has favorable geometry to fit into the 3' end of the broken DNA strand covalently linked with Top1 and the free 5'-OH end to inhibit Top1 religation activity.⁴²

To further demonstrate the importance of substitution at C-4' in compound 28, we synthesized positional analogues of 28 having -OCH₃ group at the C-2' (30) and C-3' (29) positions of the phenyl ring (Scheme 2), which were tested for

Top1 inhibitory activity. Interestingly, changing the position of the $-\text{OCH}_3$ group from C-4' to C-3' results in a slight decrease in Top1 inhibition as compound **29** shows an IC_{50} value of $1.05 \mu\text{M}$ (Table 1). These findings were noteworthy as **29** showed that suitable substitution at the C-3' position can also confer Top1 inhibition. However, compound **30** failed to show any significant Top1 inhibition at $10 \mu\text{M}$. These results underline the importance of suitable substitution at C-4' and C-3' of the phenyl group at the C-6 position of the quinoline core required for Top1 inhibition. The result prompted us to revisit the disubstitution pattern on the phenyl group at the C-6 position. In the next series of disubstituted compounds (**31**, **32**, **33**, and **34**), the position of the $-\text{OCH}_3$ group was fixed at C-4' and another $-\text{OCH}_3$ or $-\text{CH}_3$ was introduced at C-2' and C-3' positions (Scheme 2). Compounds **31** and **32** with dimethoxy substitution on the phenyl group at C-6 failed to show significant Top1 inhibition at $10 \mu\text{M}$ (Table 1). A similar result was obtained for morpholine analogue **14**. Interestingly, replacing one of the $-\text{OCH}_3$ groups at the 3' position with $-\text{CH}_3$ in **33** provided best Top1 inhibition (IC_{50} value $2.36 \mu\text{M}$) among disubstituted phenyl groups at C-6 (Table 1).

In the next development, by keeping the optimized features at C-4 and C-6 positions constant, a limited survey of the C-5'' position of the oxadiazole ring was performed by incorporating small hydrophilic and hydrophobic groups to determine the nature of substituents that can be accommodated for modulation of Top1 inhibition. Compound **36** with a hydrophilic $-\text{NH}_2$ group resulted in a drastic fall in the inhibitory activity. Installation of a small hydrophobic $-\text{CH}_3$ group at C-5'' resulted in a similar drop in Top1 activity (compound **38**). On a similar note, substituting aminopropylamino chain at C-4 with methylamine in compound **44** fails to show any Top1 inhibitory activity at $10 \mu\text{M}$. The result validated the importance of aminopropylamino side chain at the C-4 position of the quinoline core for providing significant impact on Top1 inhibition.

Our efforts to develop an acceptable hypothetical binding model that rationalize the structure–activity relationships of all the molecules resulting from minor changes in the structure proved difficult. However, molecular modeling indicates that depending on the nature of substituents at C-3, C-4, and C-6 positions of the quinoline ring, it might be capable of forming hydrogen bond interactions with important residues such as Arg364, Asn722, and Asn352 as well as stacking interactions with DA113, DC112, TGP11, and DT10 in the ternary complex. In representative compound **22** with the flexible two-carbon linker, the molecular modeling indicated that the heteroatom present in the heterocycles was unable to form a hydrogen bond with Asn352 in the major groove (Figure S2). The result signifies the importance of the length of the flexible chain containing heterocycles. Analysis of the various poses of disubstituted compounds **31** and **33** within the ternary complex revealed that the 3,4-dimethoxy phenyl group is not orientated in the same plane as observed in compound **28**. As a result, compound **31** was unable to form a hydrogen bond with Arg364 and Asn722 along with the loss in π – π stacking interactions. Interestingly, compound **33** was found to attain the stacking interactions with DA113, DC112, TGP11, and DT10 along with hydrogen bond with Arg364, which signifies the importance of specific substitutions at the C-6 position of the quinoline ring.

The structure–activity relationship signifies the importance of a perfect balance of substitution patterns at C-3, C-4, and C-

6 positions in our design. All these results together indicate the robustness of our design and rationalize the highest activity of compound **28** against Top1 in plasmid relaxation activity (Table 1). Compound **28** was selected for further lead assessment and mechanistic insight.

In Vitro ADME Study. Compounds **13** and **28** with similar structural features except for the nature of the weak basic group present at the C-4 position were evaluated in a panel of in vitro ADME assays (Tables 2 and 3). Both these

Table 2. Solubility, Plasma Stability, and log *D* Results of Potent Compounds at pH 7.4

compd	aq sol ($\mu\text{g/mL}$)	plasma stability ^a	log <i>D</i> @ pH 7.40
CPT	2.5	15.70	1.74 ^b
13	28.08 ± 0.11	83.38	3.26 ± 0.01
28	30.09 ± 0.66	93.34	2.48 ± 0.04

^aMean % remaining at 2 h in human plasma. ^blog *P* value.

Table 3. Caco-2 Permeability of Compounds **13** and **28**

compd	<i>P</i> _{app} (10^{-6} cm/s)		efflux ratio
	apical to basal	basal to apical	
13	10.89	10.98	1.02
28	7.42	11.55	1.60

compounds were found to have moderate aqueous solubility as compared to CPT. It is noteworthy to mention that both **13** and **28** demonstrated admirable human plasma stability even after 2 h, whereas CPT due to its unstable lactone was not stable. The most active compound **28** was found to be highly stable in human plasma with 93% present after 2 h. The in vitro log *D* values of **13** and **28** are 3.26 and 2.48, respectively, which are considered to be ideal for oral absorption.^{43–45} As CPT is known to be a substrate of Pgp, we examined the Caco-2 permeability for these compounds as well as the efflux ratio to evaluate whether **13** and **28** are Pgp substrates.^{46,47} To our great satisfaction, the efflux ratios of **13** and **28** are found to be <2, which signify that these compounds are not Pgp substrates. We conclude that unlike CPT, our “tailor-made” compounds **13** and **28** are highly plasma stable with an ideal log *D* value for oral absorption and are not Pgp substrates. On the basis of ADME study^{48,49} (Tables 2 and 3) and human Top1 plasmid DNA relaxation inhibition assays (Table 1), we further extend our study with compound **28** to get mechanistic insight into Top1 inhibition and evaluate its role in the anticancer activity.

Compound 28 Poisons Human Top1–DNA Cleavage Complexes. To examine the specificity of compound **28** (Figure 2A) for Top1, we used both recombinant Top1 enzyme (Figure 2B) and endogenous Top1 from the whole cell extracts of human breast adenocarcinoma (MCF7) cells^{12,20} (Figure 2C,D). When recombinant Top1 and compound **28** were added simultaneously in the plasmid DNA relaxation assays (Figure 2B, lanes 5–9), 85–90% inhibition of Top1 could be achieved at $0.1 \mu\text{M}$ concentration of compound **28** (Figure 2B, lane 7). Next, the cellular extracts were utilized as a source of Top1 (Figure 2B) for the plasmid DNA relaxation assays (ex vivo) (Figure 2C). The utility of using whole cell extract lies in the fact that the Top1 enzyme in the extract is conserved in its native structure among a plethora of other cellular proteins. The ex vivo relaxation inhibition assays with compound **28** efficiently inhibited Top1 activity when the cellular extracts were incubated with compound **28**

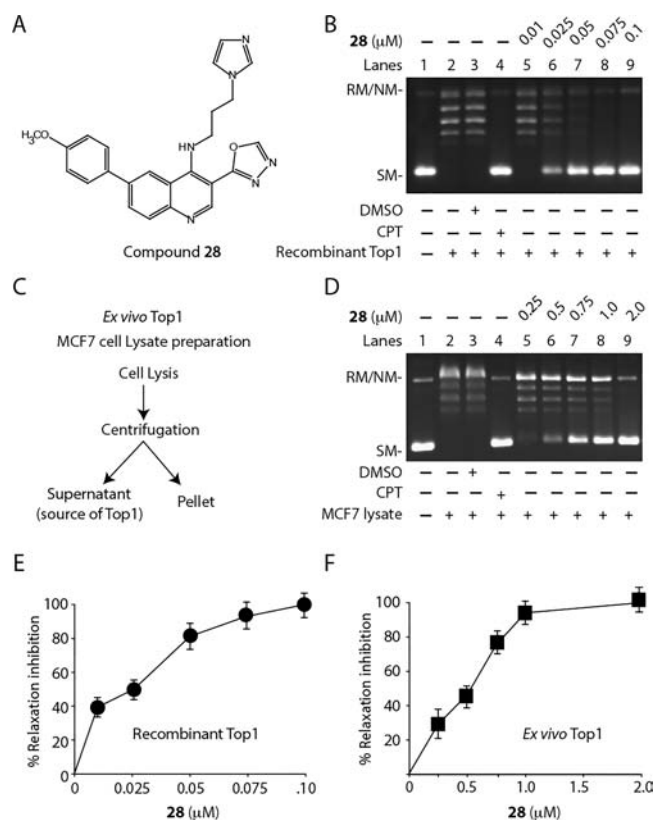


Figure 2. Inhibition of Top1-induced plasmid DNA relaxation activity by compound 28. (A) Most active compound 28. (B) Relaxation assay of supercoiled plasmid DNA using recombinant HTop1 at 3:1 molar ratio. Lane 1, pBS (SK+) DNA (90 fmol); lane 2, pBS (SK+) DNA (90 fmol) incubated with 30 fmol of recombinant Top1; lane 3, same as lane 2, additionally Top1 was incubated with 2% DMSO; lane 4, same as lane 2 but incubated simultaneously with 2 μM CPT; lanes 5–9, same as lane 2 but incubated with variable concentrations of compound 28 (as per indication) at 37 °C for 30 min. (C) Schematic representation for MCF7 whole cell lysate preparation used as the source of endogenous human Top1 for ex vivo Top1 relaxation assays. (D) Relaxation of supercoiled pBS (SK+) DNA by Top1 activity from the MCF7 cellular extract (each reaction volume contains 0.1 μg protein). Lane 1, pBS (SK+) DNA (0.3 μg); lane 2, same as lane 1, but pBS (SK+) DNA (0.3 μg) was incubated with MCF7 cell lysates; lane 3, same as lane 2 but incubated with 2% DMSO; lanes 4–9, same as lane 2, but MCF7 whole cell lysates were incubated simultaneously with 5 μM CPT or with varying concentrations of 28 (as indicated) together with plasmid DNA at 37 °C for 30 min. Positions of supercoiled monomer and nicked and relaxed monomer are indicated. (E,F) Quantitative representation of Top1 DNA relaxation inhibition (%) at variable concentrations of 28 as shown in (B,D). Recombinant Top1 (E) or endogenous Top1 from cellular extracts (F). All the experiments were performed in triplicate and expressed as the mean ± SD.

(Figure 2D, lanes 5–9) and the quantification in Figure 2E,F. Taken together, all these results indicate that compound 28 selectively inhibits human Top1, both as a recombinant enzyme (Figure 2B) and as an endogenous protein (Figure 2D), without being impaired by the pool of proteins contained in the whole cell extracts.

As both CPT and indenoisoquinolines stabilize Top1–DNA cleavable complexes (Top1cc) to inhibit Top1 activity,^{5,9,14,15,38,39,50} the mechanism of Top1 inhibition with compound 28 was investigated in the plasmid DNA cleavage assays. Closed circular DNA (form I) get converted to nicked

circular DNA (form II) by Top1 in the presence of specific inhibitors and are referred to as “cleavage complex” (Figure 3A, right panel). Figure 3A shows that compound 28 also stabilizes Top1cc formation like CPT, suggesting that compound 28 acts as a Top1 poison. We further confirmed that compound 28 is capable of stabilizing Top1cc in single turnover equilibrium cleavage assays (Figure 3B, lanes 3–8) by allowing recombinant Top1 to react with 25-mer duplex oligonucleotides modified to harbor preferred Top1 cleavage sites in the presence of indicated concentrations of compound 28 or CPT consistent with plasmid DNA cleavage assays (Figure 3A). In addition, quantification of cleavage assays (Figure 3C,D) suggests that the extent or rate of Top1–DNA cleavage complex formation (% cleavage) with compound 28 at indicated concentration is similar to CPT (Figure 3C,D). Cumulatively, our data are indicative that compound 28 is able to stabilize Top1 cleavage complexes and inhibit the religation activity with similar efficacy as that of CPT.

To investigate the ability of compound 28 to intercalate into DNA, we carried out both Top1 unwinding assays and EtBr displacement assays.^{12,40} Topoisomerase unwinding assay is based on the ability of the intercalating compounds to unwind the DNA duplex and thereby change the DNA twist. Figure 3E clearly shows that in the presence of a strong intercalative drug such as *m*-AMSA, a net negative supercoiling of the relaxed substrate DNA was induced at 50 and 200 μM concentration (Figure 3E, lanes 3 and 4). However, under similar conditions, nonintercalative compounds such as etoposide failed to show such effect at 50 and 200 μM concentrations (Figure 3E, lanes 5 and 6). Compound 28 had no effect on the topological state of the relaxed plasmid DNA at the indicated concentrations (Figure 3E, lanes 7–10), suggesting that compound 28 is not a DNA intercalator (Figure 3). Next, we further confirm that compound 28 is not a DNA intercalator by performing EtBr displacement assays. Figure 3F shows that the intercalative drug *m*-AMSA has the capability to dislodge the bound fluorophore (EtBr) at 50 μM concentration. However, nonintercalative drug such as etoposide was unable to do so. Under similar condition, compound 28 induces no displacement of fluorophore even at high concentration (200 μM) compared with the very low IC₅₀ (29 nM) of Top1 inhibition. Taken altogether, our data suggest that compound 28 is not a DNA intercalator.

Compound 28 Traps Top1 Cleavage Complexes in Live Cancer Cells. To obtain direct evidence for compound 28-mediated trapping of Top1cc (Figure 4A) in live cells, we ectopically expressed a green fluorescent-tagged human Top1 (EGFP-Top1) in MCF7 cells and tested the nuclear mobility of Top1 under live cell confocal microscopy combined with FRAP technology as described previously.^{12,51} In the absence of compound 28, FRAP recovery of EGFP-Top1 was fast (~85–90%), suggesting a large mobile population and a smaller (~10–15%) immobile population of EGFP-Top1 (Figure 4B, and the quantification in 4C; untreated). These data indicate that Top1 is mostly mobile and binds transiently with the DNA (reversible Top1cc) and are freely exchanged in the nuclear compartments.

In the presence of compound 28, the fluorescence recovery of EGFP-Top1 was markedly impeded (~55–65%) with increasing concentration of compound 28 (Figure 4B, and the quantification in 4C; (+) compound 28; 1 and 5 μM). These data suggest that compound 28 traps Top1cc on DNA in live cells like CPT,^{10,18} leading to a subsequent increase in bound/

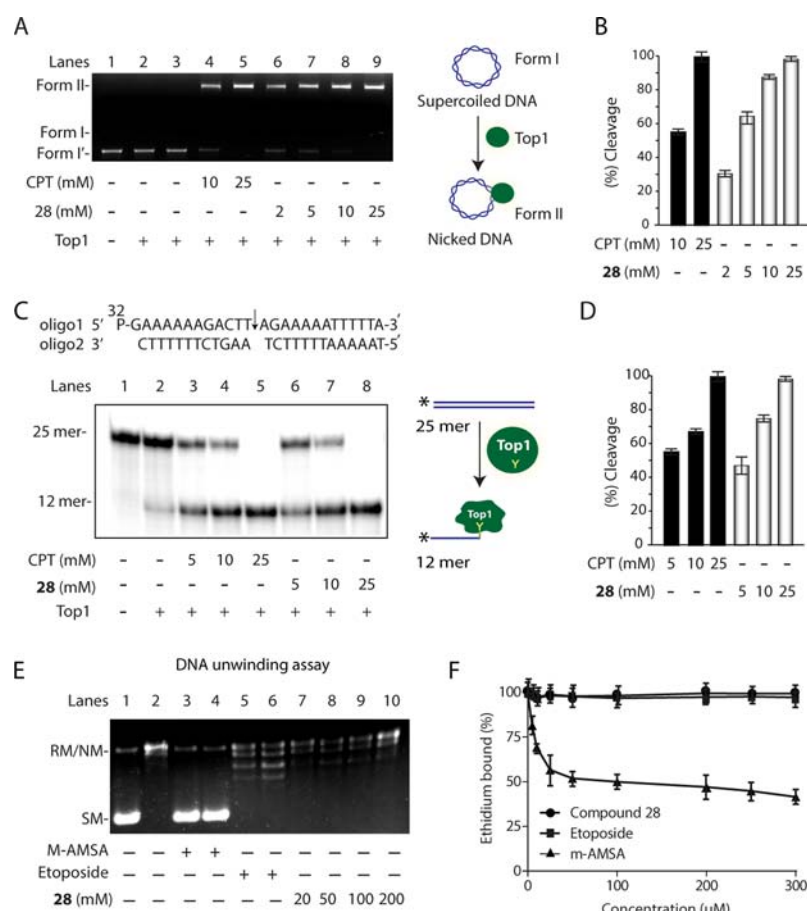


Figure 3. Compound 28-mediated trapping of Top1–DNA cleavage complexes. (A) Representative gel image depicting plasmid DNA cleavage mediated by Top1 in the presence of CPT or compound 28. Lane 1, 60 fmol of pBS (SK+) supercoiled DNA. Lanes 2–9, same as lane 1 but incubated with equal amounts of recombinant human Top1 (100 fmol) at the indicated concentrations of CPT or compound 28 or only DMSO at 37 °C for 30 min. Positions of the supercoiled substrate (form I) and nicked monomers (form II) are indicated. Schematic representation of Top1-mediated nicked DNA formation. (C) Representative gel showing Top1-mediated 25 mer duplex oligonucleotide cleavage in the presence of CPT and compound 28. Lane 1, 15 nM 5′-³²P-end labeled 25-mer duplex oligo as indicated above. Lane 2, same as lane 1 but incubated with recombinant Top1 (0.2 μM). Lanes 3–5, same as lane 2 but incubated with an indicated concentration of CPT. Lanes 6–8, same as lane 2 but incubated with an indicated concentration of compound 28. Positions of uncleaved oligonucleotide (25-mer) and the cleavage product (12-mer oligonucleotide complexed with residual Top1) are indicated. Schematic representation of the formation of 12-mer oligonucleotide attached with Top1 in the presence of Top1 poison. Quantitative measurement of cleavage complex (Top1cc) formation (%) by CPT and compound 28 either by supercoiled DNA (B) or through oligo cleavage assay (D). All the experiments were performed three times and expressed as the mean ± SD. (E) Compound 28 is not a DNA intercalator. Compound 28–DNA interaction as investigated by agarose gel electrophoresis in Top1 unwinding assays. Lane 1, 50 fmol of pBS (SK+) DNA. Lane 2, relaxed pBS (SK+) DNA generated by an excess of Top1. Lanes 3–6, same as lane 2 but incubated with 50 μM *m*-amsacrine (AMSA) and 200 μM etoposide. Lanes 7–10, same as lane 2 but incubated with 20, 50, 100, and 200 μM of compound 28 as indicated. (F) Fluorescence-based ethidium bromide displacement assay. All samples contained 1 μM EtBr and 5 nM calf thymus (CT) DNA. Graphical representation of EtBr bound (%) of increasing concentration (0–300 μM) of compound 28, *m*-AMSA, and etoposide. EtBr fluorescence was monitored with an excitation wavelength of 510 nm and an emission wavelength of 590 nm.

immobile fraction of EGFP-Top1 (Figure 4B,C), which is consistent with 28-mediated stabilization of Top1cc in the *in vitro* cleavage assays (Figure 3). The molecular modeling indicates that compound 28 possibly forms a hydrogen bonding interaction with Asn722 located in the catalytic domain of HTop1, which may contribute to the stabilization of Top1 cleavage complexes with the nicked DNA (Figure 4A). To investigate this possibility, we tested the ability of compound 28 to trap mutant Top1 at residue Asn722 (EGFP-Top1^{N722S}) in live cells by using FRAP kinetic analysis [see Figure 4D,E, panel (+) 28]. Figure 4E suggests that the FRAP recovery of EGFP-Top1^{N722S} was unaffected in the presence of increasing dosage of 28 (Figure 4D,E) and was similar to no drug treatment condition (Figure 4E), suggesting that 28 failed to trap Top1cc when Asn722 is mutated to Ser.

Taken together, these data indicate that Asn722 is critical for compound 28-mediated trapping of human Top1cc.

Compound 28 Accumulates Persistent DNA DSBs Compared to CPT. As compound 28 stabilizes Top1cc *in vitro* (Figure 3) and in live cells (Figure 4), we investigated the accumulation and disappearance of DSBs in MCF7 cells treated with compound 28 by measuring γH2AX foci formation under confocal microscopy (Figure 5), as γH2AX is a well-defined marker for Top1-mediated DSBs.^{52–57}

Under similar condition, we detected a time-dependent increase in γH2AX foci formation in cells treated with compound 28 for 3 and 5 h comparable with CPT-induced γH2AX foci at similar time periods, suggesting that both compound 28 and CPT generate similar levels of DSBs at indicated time periods in MCF7 cells (Figure 5B,C).

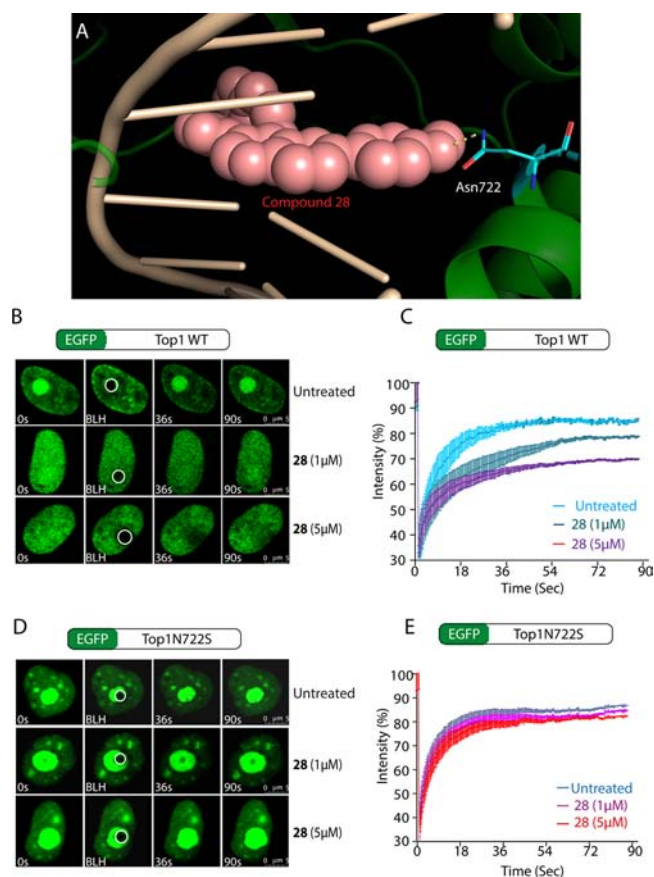


Figure 4. Compound 28-mediated stabilization of the Top1–DNA cleavage complex in live cells. (A) Space-filling model showing conservative H-bonding interaction between Asn722 and 28. (B) Compound 28 accumulates immobile/bound Top1 in the nucleus. Representative images depicting the FRAP of enhanced green fluorescent-tagged HTop1 [enhanced green fluorescent protein (EGFP)-Top1WT] transiently expressed in MCF7 cells. Cells were treated with an indicated concentration of 28 for 10 min and were analyzed by live cell spinning disk confocal microscopy and photobleaching. A subnuclear spot (ROI) indicated by a circle was bleached (BLH) for 30 ms and photographed at regular intervals of 3 ms thereafter. Successive images taken for ~90 s after bleaching illustrate fluorescence return into the bleached areas. (D) Top1N722S residue is critical for 28-induced nuclear dynamics. Representative images showing the FRAP of EGFP-Top1^{N722S} transiently expressed in MCF7 cells. Cells were treated with 28 (indicated concentration) for 10 min and were analyzed by live cell spinning disk confocal microscopy, and FRAP experiments were carried out in a similar way as with the EGFP-Top1WT. Right panels (C,E) quantification of FRAP data showing mean curves of Top1 variants in the presence and absence of 28. Error bars represent mean \pm SE ($n = 15$).

CPT-induced γ H2AX have a short half-life as they are reversible immediately after a wash,^{52,54} which is consistent with the reversal of Top1cc intermediates within minutes after washing out CPT.⁵⁸ Next, to test the ability of compound 28 to induce more persistent and less reversible DNA breaks, we investigated the disappearance of γ H2AX in cells treated with compound 28 and compared it with CPT after subsequent wash and culture in the drug-free medium for indicated time periods (Figure 5A). In Figure 5B, the right panel shows faster disappearance of γ H2AX foci after washing out CPT from media at indicated time periods (see the quantification in Figure 5C). In contrast, cells showed (3–4 fold) more

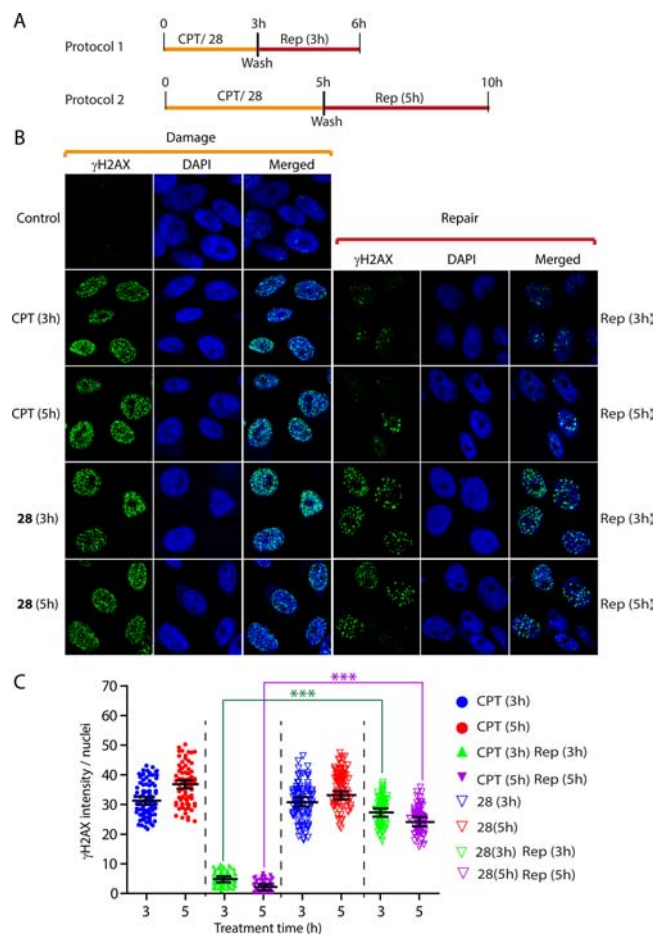


Figure 5. Compound 28 generates persistent and less reversible DNA DSBs as detected by γ H2AX staining. (A) Overview for the protocol of drug treatment and reversal in MCF7 cells. (B) Time-dependent accumulation of γ H2AX foci formation in MCF7 cells treated with compound 28 or CPT for 3 and 5 h and reversal of γ H2AX foci after drug removal for indicated times. (C) Quantification of γ H2AX intensity per nucleus after treatment and after the removal of indicated inhibitors (compound 28 or CPT) obtained from immunofluorescence confocal microscopy was calculated for 35–40 cells (mean \pm SEM) and plotted as a function of time (h).

persistent γ H2AX foci (Figure 5B, right panel and the quantification in Figure 5C) even after washing out compound 28 at the indicated time. Figure 5C further indicates that γ H2AX foci were persistent for 5 h after drug removal in compound 28-treated cells. Taken together, our data suggest that compound 28 generates more persistent and less reversible Top1cc-induced DSBs compared to CPT.

Compound 28 Exhibits Potent Anticancer Activity.

Compound 28 was evaluated for its cytotoxicity in the cancer cell lines from different tissue origin.⁵² Cytotoxicity assays were performed in human breast adenocarcinoma cell lines (MCF7), human cervical cancer cell lines (HeLa), human colon carcinoma cell lines (HCT116), human ovarian adenocarcinoma cell lines (NIH:OVCA-3), as well as noncancerous human embryonic kidney (HEK293) cells with variable concentrations of compound 28. Table S2 (Supporting Information) indicates that compound 28 revealed cytotoxicity in cancerous cells including MCF7 (IC_{50} : 2.74 μ M), HeLa (IC_{50} : 2.61 μ M), HCT116 (IC_{50} : 2.34 μ M), and

NIH:OVCAR-3 (IC_{50} : 2.35 μ M) cells compared to the noncancerous cells such as HEK293 (IC_{50} : 8.34 μ M).

TDP1 hydrolyzes the phosphodiester bond at a DNA 3'-end linked to a tyrosyl moiety of stalled Top1-DNA covalent complexes; therefore, TDP1-/- cells are hypersensitive toward Top1 poisons.^{51–54,59,60} With further evidence for the poisoning of Top1cc with compound **28** and hypersensitivity in DNA repair-deficient cells, we have performed cytotoxicity assays with TDP1-/- (IC_{50} : 1.02 μ M) and TDP1+/+ MEFs (IC_{50} : 2.91 μ M) cells in the presence of compound **28**. Table S2 indicates that TDP1-/- MEFs cells were hypersensitive to compound **28**, further providing evidence that compound **28** induces cytotoxicity by stabilizing Top1cc in cells. Taken together, all data confirm that compound **28** is a potent Top1 poison and is a potential candidate as an anticancer chemotherapeutic agent.

CONCLUSIONS

As CPT and its clinically approved drugs suffer from several limitations, there is a great interest in the development of “non-CPT” Top1 poisons as anticancer agents. In the present study, we successfully report a novel class of Top1 poisons based on the quinoline core through an understanding of the structural features of ligands essential for binding in the active site. The design signifies the importance of a perfect balance of substitution patterns at C-3, C-4, and C-6 positions of the quinoline core. Most potent compound **28** stabilizes Top1cc in vitro and in live cells to inhibit the religation activity without intercalating to the DNA with similar efficacy as that of CPT. The mechanistic insight through the FRAP assay of compound **28**-mediated trapping of human Top1cc revealed the significance of Asn722, an important amino acid residue at the active site. Unlike CPT, compound **28** generates less reversible DNA DSBs because of the accumulation of irreversible Top1cc-induced DSBs. In vitro ADME study revealed that unlike CPT and its derivatives, compound **28** is highly plasma stable with ideal log *D* value for oral absorption and is not a Pgp substrate. In summary, we provide compelling evidence that advocate compound **28** as a potential anticancer agent.

EXPERIMENTAL SECTION

Chemistry. General Methods. All starting materials, reagents, and solvents were purchased from commercial suppliers and used without further purification. Air-sensitive reactions were carried out under dry nitrogen or argon atmosphere. Solvents were distilled before use and also dried using standard methods. Thin-layer chromatography was performed on silica gel plates (Merck Silica Gel 60, F₂₅₄), and the spots were visualized under UV light (254 and 365 nm) or by charring the plate dipped in ninhydrin or KMnO₄ or vanillin solution. For purification of the compounds along with manual column flash chromatography was also performed with RediSep Rf silica gel columns on the Teledyne ISCO CombiFlash Rf system using 230–400 mesh silica gel. ¹H NMR was recorded at 300 MHz (Bruker DPX), 400 MHz (Jeol), and 600 MHz (Bruker Avance) frequency, and ¹³C NMR spectra were recorded at 75 MHz (Bruker DPX), 100 MHz (Jeol), and 150 MHz (Bruker Avance) frequency in CDCl₃ or CD₃OD or DMSO-*d*₆ solvent using tetramethylsilane (TMS) as the internal standard. Chemical shifts were measured in parts per million (ppm) referenced to 0.0 ppm for TMS and 7.260 ppm for CHCl₃. The following abbreviations were used to explain multiplicities: s = singlet, d = doublet, t = triplet, q = quartet, m = multiplet, br = broad. Coupling constant, *J*, was reported in hertz unit. High-resolution mass spectra, HRMS (*m/z*), were recorded using electron ionization (Jeol-JMS 700 mass spectrometer) and electrospray ionization (ESI; Q-ToF

Micro mass spectrometer and LTQ Orbitrap XL mass spectrometer) techniques. The purity of the selected compounds was analyzed by Hitachi HPLC using column Xtimate C18 (4.6 × 150 mm 5.0 μ m). The HPLC purity of all the compounds subjected to biological assay is >95%.

Ethyl 6-Bromo-4-chloroquinoline-3-carboxylate (1). Ethyl 6-bromo-4-hydroxyquinoline-3-carboxylate (2 g, 6.75 mmol) was taken in POCl₃ (15 mL) in ice-cold condition. The reaction mixture was allowed to come to room temperature and heated for 2 h at 100 °C. The reaction mixture was poured into crushed ice and neutralized with a saturated sodium bicarbonate solution. The organic part was extracted with ethyl acetate, washed with water and brine, concentrated, and dried. The solid was purified by silica gel flash column chromatography, eluting with 15% ethyl acetate in hexane to give compound **1** as a white crystalline solid (1.8 g, 85% yield). ¹H NMR (300 MHz, CDCl₃): δ 9.2 (s, 1H), 8.58 (d, *J* = 2.4 Hz, 1H), 8.02 (d, *J* = 9.3 Hz, 1H), 7.92 (dd, *J* = 9.0, 1.8 Hz, 1H), 4.51 (q, *J* = 7.5 Hz, 2H), 1.47 (t, *J* = 7.5 Hz, 3H). MS (ESI) *m/z*: [M + Na]⁺ 338.16.

General Procedure A. Ethyl 6-Bromo-4-(2-morpholinoethylamino)quinoline-3-carboxylate (2). Compound **1** (1 g, 3.18 mmol) was dissolved in 1,4-dioxane (5 mL) under N₂ atmosphere. To the reaction mixture, dry DIPEA (1.11 mL, 6.36 mmol) and 4-(2-aminoethyl)morpholine (0.63 mL, 4.77 mmol) were added. The reaction mixture was allowed to stir for 12 h at room temperature. It was then poured into 50 mL of water. The solid obtained was filtered and purified by column chromatography to give compound **2** as a white solid (1.1 g, 85% yield). ¹H NMR (300 MHz, CDCl₃): δ 9.51 (br s, -NH), 9.1 (s, 1H), 8.4 (d, *J* = 1.5 Hz, 1H), 7.83 (d, *J* = 9.0 Hz, 1H), 7.73 (dd, *J* = 8.7, 1.8 Hz, 1H), 4.41 (q, *J* = 7.2 Hz, 2H), 3.92–3.87 (m, 2H), 3.78 (t, *J* = 4.5 Hz, 4H), 2.71 (t, *J* = 6.0 Hz, 2H), 2.57 (t, *J* = 4.2 Hz, 4H), 1.44 (t, *J* = 7.5 Hz, 3H). ¹³C NMR (150 MHz, CDCl₃): δ 168.0, 155.7, 152.0, 149.8, 134.0, 131.6, 128.2, 120.9, 117.2, 103.8, 67.0, 60.7, 58.0, 53.3, 45.4, 14.4. MS (ESI) *m/z*: [M + H]⁺ 410.35. HRMS (EI) *m/z*: [M]⁺ calcd for C₁₈H₂₂BrN₃O₃, 407.0845; found, 407.0852.

Ethyl 6-Bromo-4-(3-morpholinopropylamino)quinoline-3-carboxylate (3). Compound **1** (1 g, 3.18 mmol) was dissolved in 1,4-dioxane (5 mL) under N₂ atmosphere. To the reaction mixture, dry DIPEA (1.11 mL, 6.36 mmol) and 3-morpholinopropan-1-amine (0.63 mL, 4.77 mmol) were added, and the reaction was performed according to general procedure A. The solid obtained was filtered and dried to give compound **3** as a white solid (1.2 g, 90% yield). ¹H NMR (300 MHz, CDCl₃): δ 9.23 (br s, -NH), 9.06 (s, 1H), 8.36 (d, *J* = 2.1 Hz, 1H), 7.81 (d, *J* = 9.0 Hz, 1H), 7.72 (dd, *J* = 9.0, 2.1 Hz, 1H), 4.38 (q, *J* = 7.2 Hz, 2H), 3.87–3.81 (m, 2H), 3.69 (t, *J* = 4.5 Hz, 4H), 2.50 (t, *J* = 7.2 Hz, 2H), 2.44 (t, *J* = 4.5 Hz, 4H), 1.99–1.90 (m, 2H), 1.42 (t, *J* = 7.2 Hz, 3H). ¹³C NMR (100 MHz, CDCl₃): δ 168.7, 156.1, 152.0, 149.8, 134.3, 131.6, 128.3, 120.9, 117.5, 103.5, 67.0, 61.0, 56.0, 53.8, 46.9, 27.8, 14.4. ESI-MS *m/z*: [M + H]⁺ 422.30. HRMS *m/z*: [M + H]⁺ calcd for C₁₉H₂₅BrN₃O₃, 422.1079; found, 422.1072.

General Procedure B. 6-Bromo-4-(2-morpholinoethylamino)quinoline-3-carbohydrazide (4). Compound **2** (1 g, 2.45 mmol) was dissolved in ethanol (10 mL). To the solution, hydrazine hydrate (10 mL) was added. The reaction mixture was stirred for 10 h at room temperature. Ethanol was removed under vacuum. The residue was then dissolved in CHCl₃, and the organic layer was washed with water and brine, dried, and concentrated to give compound **4** as a yellow solid (0.6 g, 62% yield). mp > 250 °C. ¹H NMR (300 MHz, CDCl₃): δ 8.64 (s, 1H), 8.27 (d, *J* = 1.5 Hz, 1H), 7.84 (d, *J* = 8.7 Hz, 1H), 7.73 (dd, *J* = 8.7, 1.5 Hz, 1H), 3.77 (t, *J* = 4.8 Hz, 4H), 3.70–3.65 (m, 2H), 2.68 (t, *J* = 6.3 Hz, 2H), 2.54 (t, *J* = 4.2 Hz, 4H). ¹³C NMR (100 MHz, CDCl₃): δ 169.2, 152.3, 149.1, 148.3, 133.7, 131.2, 126.6, 121.2, 118.2, 107.8, 67.0, 57.7, 53.2, 44.1, 31.6, 22.7. ESI-MS *m/z*: [M + H]⁺ 394.41. HRMS *m/z*: [M + H]⁺ calcd for C₁₆H₂₁BrN₅O₂, 394.0878; found, 398.0874.

6-Bromo-4-(3-morpholinopropylamino)quinoline-3-carbohydrazide (5). Compound **3** (1 g, 2.37 mmol) was dissolved in ethanol (10 mL). To the solution, hydrazine hydrate (10 mL) was added. The

reaction was performed according to general procedure B. The residue was dissolved in CHCl_3 , and the organic layer was washed with water and brine, dried, and concentrated to give compound **5** (0.85 g, 88% yield) as a pale yellow solid. mp > 250 °C. ^1H NMR (300 MHz, CD_3OD): δ 8.48 (d, J = 2.1 Hz, 1H), 8.40 (s, 1H), 7.82 (dd, J = 8.7 Hz, 1H), 7.74 (d, J = 9.0 Hz, 1H), 3.76 (t, J = 4.5 Hz, 4H), 3.71 (t, J = 4.8 Hz, 2H), 3.56 (t, J = 6.6 Hz, 2H), 2.52–2.50 (m, 4H), 1.96–1.87 (m, 2H). ^{13}C NMR (100 MHz, CD_3OD): δ 169.1, 149.9, 148.6, 146.7, 134.5, 133.4, 129.8, 121.0, 118.5, 108.2, 66.3, 57.0, 53.6, 53.4, 46.3, 44.9, 25.4. ESI-MS m/z : $[\text{M} + \text{H}]^+$ 408.20. HRMS m/z : $[\text{M} + \text{H}]^+$ calcd for $\text{C}_{17}\text{H}_{23}\text{BrN}_5\text{O}_2$, 408.1035; found, 408.1030.

6-Bromo-N-(2-morpholinoethyl)-3-(1,3,4-oxadiazol-2-yl)-quinolin-4-amine (6). Compound **4** (1 g, 2.54 mmol) was taken in triethyl orthoformate (5 mL, 30.06 mmol), and the mixture was heated for 12 h at 110 °C. The reaction mixture was allowed to come to room temperature. Excess hexane was added to the mixture. A precipitation formed was filtered and purified by column chromatography, eluting with 1% methanol in CHCl_3 to give compound **6** as a light yellow solid (0.4 g, 39% yield). mp 180 °C. ^1H NMR (300 MHz, CDCl_3): δ 9.22 (br s, –NH), 9.03 (s, 1H), 8.47 (m, 2H), 7.86 (d, J = 8.7 Hz, 1H), 7.75 (dd, J = 8.7, 1.8 Hz, 1H), 4.00–3.95 (m, 2H), 3.77 (t, J = 4.5 Hz, 4H), 2.74 (t, J = 6.0 Hz, 2H), 2.58 (t, J = 4.5 Hz, 4H). ^{13}C NMR (150 MHz, CDCl_3): δ 163.5, 151.4, 151.0, 149.2, 148.7, 134.0, 131.7, 128.0, 120.5, 117.8, 99.2, 67.0, 57.9, 53.3, 45.8. MS (ESI) m/z : $[\text{M} + \text{H}]^+$ 404.37. HRMS (EI) m/z : $[\text{M}]^+$ calcd for $\text{C}_{17}\text{H}_{18}\text{BrN}_5\text{O}_2$, 403.0644; found, 403.0635.

6-Bromo-3-(5-methyl-1,3,4-oxadiazol-2-yl)-N-(2-morpholinoethyl)quinolin-4-amine (7). Compound **4** (0.15 g, 0.38 mmol) was dissolved in ethanol (3 mL), and to the solution, triethyl orthoacetate (3 mL, 16.37 mmol) was added. The reaction mixture was refluxed for 8 h. The reaction mixture was allowed to come to room temperature, and solvent was evaporated. Excess hexane was added to the mixture. A precipitation formed was filtered and purified by column chromatography, eluting with 3% methanol in CHCl_3 to give compound **7** (0.14 g, 88% yield) as a brown solid. mp 230 °C. ^1H NMR (300 MHz, CDCl_3): δ 9.17 (br s, –NH), 8.99 (s, 1H), 8.48 (d, J = 1.8 Hz, 1H), 7.86 (d, J = 8.7 Hz, 1H), 7.74 (dd, J = 8.7, 2.1 Hz, 1H), 4.00–3.94 (m, 2H), 3.78 (t, J = 4.5 Hz, 4H), 2.75 (t, J = 6.0 Hz, 2H), 2.68 (s, 3H), 2.59 (t, J = 4.5 Hz, 4H). ^{13}C NMR (100 MHz, CDCl_3): δ 163.8, 162.2, 151.3, 148.6, 133.8, 131.7, 128.0, 120.7, 117.8, 99.7, 67.1, 58.1, 53.4, 45.9, 11.1. ESI-MS m/z : $[\text{M} + \text{H}]^+$ 418.37. HRMS m/z : $[\text{M} + \text{H}]^+$ calcd for $\text{C}_{18}\text{H}_{21}\text{BrN}_5\text{O}_2$, 418.0878; found, 408.0880.

General Procedure C. 6-(4-Methoxyphenyl)-N-(2-morpholinoethyl)-3-(1,3,4-oxadiazol-2-yl)quinolin-4-amine (8). Compound **6** (0.15 g, 0.37 mmol) was dissolved in 1,4-dioxane (5 mL) under Ar atmosphere. 2-(4-Methoxyphenyl)-4,4,5,5-tetramethyl-1,3,2-dioxaborolane (0.17 g, 0.74 mmol) was added to the mixture. 2(M) Na_2CO_3 solution (0.5 mL) was added to the reaction mixture, and argon was purged for 15 min. $\text{Pd}(\text{PPh}_3)_4$ (0.035 g, 0.03 mmol) was added to the mixture, and argon purging was performed for 15 min. The mixture was heated for 12 h at 100 °C. 1,4-Dioxane was removed under vacuum, the residue was dissolved in CHCl_3 , and the organic layer was washed with water and brine, dried, and concentrated. The residue was purified by silica gel column chromatography to produce compound **8** as a white solid (0.09 g, 56% yield). mp 156 °C. ^1H NMR (600 MHz, CDCl_3): δ 9.05 (s, 1H), 8.49 (s, 1H), 8.45 (d, J = 1.2 Hz, 1H), 8.06 (d, J = 8.4 Hz, 1H), 7.94 (dd, J = 8.4, 1.2 Hz, 1H), 7.62 (d, J = 9.0 Hz, 2H), 7.05 (d, J = 8.4 Hz, 2H), 4.10–4.07 (m, 2H), 3.89 (s, 3H), 3.77 (t, J = 4.8 Hz, 4H), 2.76 (t, J = 6.0 Hz, 2H), 2.58 (br s, 4H). ^{13}C NMR (75 MHz, CDCl_3): δ 163.7, 159.4, 152.6, 150.9, 149.2, 148.0, 136.9, 132.8, 130.1, 130.0, 128.2, 122.9, 119.5, 114.4, 98.9, 67.0, 58.0, 55.4, 53.2, 46.0. MS (ESI) m/z : $[\text{M} + \text{H}]^+$ 432.42. HRMS (FAB) m/z : $[\text{M} + \text{H}]^+$ calcd for $\text{C}_{24}\text{H}_{26}\text{N}_5\text{O}_3$, 432.2035; found, 432.2053. HPLC purity 99.55%.

6-(3,4-Dimethoxyphenyl)-N-(2-morpholinoethyl)-3-(1,3,4-oxadiazol-2-yl)quinolin-4-amine (9). Compound **6** (0.10 g, 0.25 mmol) was taken along with 3,4-dimethoxyphenylboronic acid (0.091 g, 0.5 mmol) in 1,4-dioxane (5 mL). 2(M) Na_2CO_3 solution (0.3 mL) and

$\text{Pd}(\text{PPh}_3)_4$ (0.023 g, 0.02 mmol) were added to the mixture, and the reaction was performed according to procedure A. The reaction mixture was heated at 90 °C for 12 h. The residue was purified by column chromatography, eluting with 5% methanol in CHCl_3 to give compound **9** as a yellow solid (0.035 g, 31% yield). mp 116 °C. ^1H NMR (300 MHz, CDCl_3): δ 9.21 (br s, –NH), 9.06 (s, 1H), 8.51 (s, 1H), 8.45 (d, J = 1.5 Hz, 1H), 8.07 (d, J = 8.7 Hz, 1H), 7.93 (dd, J = 8.7, 1.8 Hz, 1H), 7.25 (dd, J = 8.7, 1.8 Hz, 1H), 7.19 (d, J = 2.1 Hz, 1H), 7.03 (d, J = 8.4 Hz, 1H), 4.11–4.06 (m, 2H), 4.01 (s, 3H), 3.98 (s, 3H), 3.77 (t, J = 4.5 Hz, 4H), 2.76 (t, J = 6.0 Hz, 2H), 2.58 (t, J = 4.5 Hz, 4H). ^{13}C NMR (150 MHz, CDCl_3): δ 163.7, 152.9, 151.0, 149.4, 149.1, 148.9, 147.8, 137.5, 133.4, 130.5, 129.8, 123.3, 119.7, 119.5, 111.7, 110.6, 99.1, 67.0, 58.1, 56.1, 53.3, 46.1. MS (ESI) m/z : $[\text{M} + \text{H}]^+$ 461.51. HRMS (EI) m/z : $[\text{M}]^+$ calcd for $\text{C}_{25}\text{H}_{27}\text{N}_5\text{O}_4$, 461.2063; found, 461.2051. HPLC purity 99.27%.

6-(4-Methoxyphenyl)-3-(5-methyl-1,3,4-oxadiazol-2-yl)-N-(2-morpholinoethyl)quinolin-4-amine (10). Compound **7** (0.075 g, 0.18 mmol) was taken along with 2-(4-methoxyphenyl)-4,4,5,5-tetramethyl-1,3,2-dioxaborolane (0.17 g, 0.36 mmol) in 1,4-dioxane (5 mL). 2(M) Na_2CO_3 solution (0.23 mL) and $\text{Pd}(\text{PPh}_3)_4$ (0.017 g, 0.014 mmol) were added to the mixture, and the reaction was performed according to procedure A. The residue was purified by silica gel column chromatography, eluting with 2% methanol in CHCl_3 to afford compound **10** as an off-white solid (0.025 g, 31% yield). mp 160 °C. ^1H NMR (300 MHz, CDCl_3): δ 9.14 (br s, –NH), 8.99 (s, 1H), 8.44 (d, J = 1.5 Hz, 1H), 8.05 (d, J = 8.7 Hz, 1H), 7.92 (dd, J = 8.7, 1.5 Hz, 1H), 7.63 (d, J = 8.7 Hz, 2H), 7.05 (d, J = 8.7 Hz, 2H), 4.09–4.04 (m, 2H), 3.90 (s, 3H), 3.76 (t, J = 4.5 Hz, 4H), 2.75 (t, J = 6.0 Hz, 2H), 2.69 (s, 3H), 2.57 (t, J = 4.2 Hz, 4H). ^{13}C NMR (75 MHz, CDCl_3): δ 164.0, 162.0, 159.5, 152.6, 147.8, 137.0, 133.0, 130.1, 128.3, 123.0, 119.7, 116.2, 114.5, 99.5, 67.1, 58.2, 55.4, 53.3, 46.2, 11.0. MS (ESI) m/z : $[\text{M} + \text{H}]^+$ 446.50. HRMS (EI) m/z : $[\text{M}]^+$ calcd for $\text{C}_{25}\text{H}_{27}\text{N}_5\text{O}_4$, 445.2114; found, 445.2112. HPLC purity 96.96%.

6-(3,4-Dimethoxyphenyl)-3-(5-methyl-1,3,4-oxadiazol-2-yl)-N-(2-morpholinoethyl)quinolin-4-amine (11). Compound **7** (0.065 g, 0.16 mmol) was taken along with 3,4-dimethoxyphenylboronic acid (0.073 g, 0.4 mmol) in 1,4-dioxane (5 mL). 2(M) Na_2CO_3 solution (0.3 mL) and $\text{Pd}(\text{PPh}_3)_4$ (0.015 g, 0.013 mmol) were added to the mixture, and the reaction was performed according to general procedure A. Purification was done by silica gel column chromatography, eluting with 3% methanol in CHCl_3 to get compound **11** as a light yellow solid (0.03 g, 41% yield). mp 180 °C. ^1H NMR (300 MHz, CDCl_3): δ 9.11 (br s, –NH), 8.99 (s, 1H), 8.42 (s, 1H), 8.05 (d, J = 8.7 Hz, 1H), 7.90 (dd, J = 8.4, 1.5 Hz, 1H), 7.24 (dd, J = 8.1, 1.5 Hz, 1H), 7.17 (d, J = 1.5 Hz, 1H), 7.01 (d, J = 8.4 Hz, 1H), 4.08–4.03 (m, 2H), 3.99 (s, 3H), 3.96 (s, 3H), 3.75 (t, J = 4.5 Hz, 4H), 2.74 (t, J = 6.0 Hz, 2H), 2.68 (s, 3H), 2.56 (t, J = 4.5 Hz, 4H). ^{13}C NMR (75 MHz, CDCl_3): δ 164.0, 162.0, 152.6, 149.4, 149.0, 148.0, 137.2, 133.6, 130.2, 130.1, 123.3, 119.7, 111.7, 110.6, 99.6, 67.1, 58.3, 56.1, 53.3, 46.2, 11.0. MS (ESI) m/z : $[\text{M} + \text{H}]^+$ 476.58. HRMS (EI) m/z : $[\text{M}]^+$ calcd for $\text{C}_{25}\text{H}_{27}\text{N}_5\text{O}_4$, 475.2220; found, 475.2226. HPLC purity 96.38%.

6-Bromo-N-(3-morpholinopropyl)-3-(1,3,4-oxadiazol-2-yl)-quinolin-4-amine (12). Compound **5** (1 g, 2.45 mmol) was taken in triethyl orthoformate (5 mL, 30.06 mmol), and the mixture was heated for 12 h at 110 °C. The crude mixture was purified by column chromatography, eluting with 4% methanol in CHCl_3 to give compound **12** as a yellow solid (0.25 g, 25% yield). mp 144 °C. ^1H NMR (300 MHz, CDCl_3): δ 9.03 (s, 1H), 8.82 (br s, –NH), 8.49 (s, 1H), 8.46 (d, J = 0.9 Hz, 1H), 7.86 (d, J = 8.7 Hz, 1H), 7.76 (dd, J = 9.0, 1.8 Hz, 1H), 3.99–3.93 (m, 2H), 3.70 (t, J = 4.5 Hz, 4H), 2.54 (t, J = 6.9 Hz, 2H), 2.45 (t, J = 3.9 Hz, 4H), 2.08–1.99 (m, 2H). ^{13}C NMR (75 MHz, CDCl_3): δ 163.8, 151.6, 151.0, 149.1, 148.7, 134.1, 131.7, 128.0, 120.4, 118.0, 98.9, 66.9, 55.7, 53.7, 46.9, 27.7. MS (ESI) m/z : $[\text{M} + \text{H}]^+$ 418.31. HRMS m/z : $[\text{M} + \text{H}]^+$ calcd for $\text{C}_{18}\text{H}_{21}\text{BrN}_5\text{O}_2$, 418.0878; found, 418.0862.

6-(4-Methoxyphenyl)-N-(3-morpholinopropyl)-3-(1,3,4-oxadiazol-2-yl)quinolin-4-amine (13). Compound **12** (0.10 g, 0.24 mmol) was taken along with 2-(4-methoxyphenyl)-4,4,5,5-tetramethyl-1,3,2-

dioxaborolane (0.11 g, 0.48 mmol) in 1,4-dioxane (5 mL). 2(M) Na_2CO_3 solution (0.3 mL) and $\text{Pd}(\text{PPh}_3)_4$ (0.022 g, 0.019 mmol) were added to the mixture, and the reaction was performed according to procedure A. The residue was purified by silica gel column chromatography to produce compound 13 as a gray solid (0.037 g, 35% yield). mp 134 °C. ^1H NMR (600 MHz, CDCl_3): δ 9.06 (s, 1H), 8.86 (br s, -NH), 8.51 (s, 1H), 8.47 (d, J = 1.2 Hz, 1H), 8.08 (d, J = 9.0 Hz, 1H), 7.96 (dd, J = 9.0, 1.8 Hz, 1H), 7.64 (d, J = 9.0 Hz, 2H), 7.07 (d, J = 8.4 Hz, 2H), 4.13–4.10 (m, 2H), 3.91 (s, 3H), 3.69 (t, J = 4.2 Hz, 4H), 2.57 (t, J = 7.2 Hz, 2H), 2.47 (s, 4H), 2.12–2.07 (m, 2H). ^{13}C NMR (150 MHz, CDCl_3): δ 164.1, 159.6, 153.0, 150.9, 149.2, 147.9, 137.2, 133.0, 130.4, 130.2, 128.3, 123.2, 119.5, 114.6, 98.8, 66.8, 55.8, 55.5, 53.7, 47.3, 27.9. MS (ESI) m/z : $[\text{M} + \text{H}]^+$ 446.39. HRMS (ESI) m/z : $[\text{M} + \text{H}]^+$ calcd for $\text{C}_{25}\text{H}_{28}\text{N}_5\text{O}_3$, 446.2192; found, 446.2190. HPLC purity 98.23%.

6-(3,4-Dimethoxyphenyl)-N-(3-morpholinopropyl)-3-(1,3,4-oxadiazol-2-yl)quinolin-4-amine (14). Compound 12 (0.10 g, 0.24 mmol) was taken along with 3,4-dimethoxyphenylboronic acid (0.087 g, 0.48 mmol) in a mixture of 1,4-dioxane (4 mL) and dimethylformamide (DMF) (1 mL). 2(M) Na_2CO_3 solution (0.3 mL) and $\text{Pd}(\text{PPh}_3)_4$ (0.022 g, 0.02 mmol) were added to the mixture, and the reaction was performed according to procedure A. The residue was purified by silica gel column chromatography to afford compound 14 as a white solid (0.033 g, 30% yield). mp 182 °C. ^1H NMR (300 MHz, CD_3OD): δ 9.08 (s, 1H), 8.93 (s, 1H), 8.58 (s, 1H), 8.08 (dd, J = 9.0, 1.5 Hz, 1H), 7.97 (d, J = 8.7 Hz, 1H), 7.35–7.34 (m, 2H), 7.12 (d, J = 9.3 Hz, 1H), 4.09 (t, J = 6.9 Hz, 2H), 3.97 (s, 3H), 3.92 (s, 3H), 3.64 (t, J = 4.8 Hz, 4H), 2.60 (t, J = 6.9 Hz, 2H), 2.49 (t, J = 3.9 Hz, 4H), 2.11–2.07 (m, 2H). ^{13}C NMR (150 MHz, CDCl_3): δ 164.2, 152.9, 150.9, 149.6, 149.4, 149.0, 148.2, 137.3, 133.5, 130.4, 123.4, 119.6, 119.5, 111.7, 110.5, 98.8, 66.9, 56.1, 55.8, 53.7, 47.3, 28.1. MS (ESI) m/z : $[\text{M} + \text{H}]^+$ 476.37. HRMS (ESI) m/z : $[\text{M} + \text{H}]^+$ calcd for $\text{C}_{25}\text{H}_{28}\text{N}_5\text{O}_3$, 476.2298; found, 476.2291. HPLC purity 99.67%.

N-(3-Morpholinopropyl)-3-(1,3,4-oxadiazol-2-yl)-6-(p-tolyl)-quinolin-4-amine (15). Compound 12 (0.10 g, 0.24 mmol) was taken along with *p*-tolylboronic acid (0.049 g, 0.36 mmol) in 1,4-dioxane (5 mL). 2(M) Na_2CO_3 solution (0.3 mL) and $\text{Pd}(\text{PPh}_3)_4$ (0.023 g, 0.02 mmol) were added to the mixture, and the reaction was performed according to procedure A. The reaction took 8 h to complete. The residue was purified by silica gel column chromatography to produce compound 15 as a white solid (0.039 g, 38% yield). mp 168 °C. ^1H NMR (300 MHz, CDCl_3): δ 9.04 (s, 1H), 8.82 (br s, -NH), 8.48 (s, 2H), 8.05 (d, J = 8.7 Hz, 1H), 7.95 (d, J = 8.4 Hz, 1H), 7.58 (d, J = 7.8 Hz, 2H), 7.32 (d, J = 7.5 Hz, 2H), 4.11–4.05 (m, 2H), 3.64 (t, J = 4.5 Hz, 4H), 2.52 (t, J = 7.2 Hz, 2H), 2.44–2.42 (m, 7H), 2.09–2.01 (m, 2H). ^{13}C NMR (75 MHz, CDCl_3): δ 165.1, 152.9, 150.8, 148.1, 143.5, 137.7, 137.4, 130.4, 129.8, 127.1, 123.7, 123.6, 66.9, 55.8, 53.7, 47.3, 28.0, 21.1. MS (ESI) m/z : $[\text{M} + \text{H}]^+$ 430.41. HRMS m/z : $[\text{M} + \text{H}]^+$ calcd for $\text{C}_{25}\text{H}_{28}\text{N}_5\text{O}_2$, 430.2243; found, 430.2240. HPLC purity 98.89%.

Ethyl 4-(2-(1H-imidazol-1-yl)ethylamino)-6-bromoquinoline-3-carboxylate (16). Compound 1 (0.5 g, 1.59 mmol) was dissolved in 1,4-dioxane (2.5 mL) and DMF (1 mL) under N_2 atmosphere. To the reaction mixture, dry DIPEA (0.55 mL, 3.18 mmol) and 2-(1H-imidazol-1-yl)ethanamine (0.27 g, 2.39 mmol) were added. The reaction mixture was heated for 12 h at 100 °C. 1,4-Dioxane and DMF were removed under vacuum, the residue was dissolved in $\text{CHCl}_3/\text{MeOH}$ mixture, and the organic layer was washed with water and brine, dried, and concentrated. The residue was purified by silica gel column chromatography, eluting with 4% methanol in CHCl_3 to produce compound 16 as a yellow solid (0.35 g, 57% yield). mp 218 °C. ^1H NMR (600 MHz, $\text{DMSO}-d_6$): δ 8.79 (s, 1H), 8.45 (s, 1H), 8.35 (br s, -NH), 7.85 (dd, J = 9.0, 1.8 Hz, 1H), 7.76 (d, J = 9 Hz, 1H), 7.58 (s, 1H), 7.13 (s, 1H), 6.80 (s, 1H), 4.33–4.30 (m, 4H), 3.89–3.88 (m, 2H), 1.32 (t, J = 7.2 Hz, 3H). ^{13}C NMR (150 MHz, CDCl_3): δ 168.4, 155.8, 151.6, 149.7, 134.5, 131.9, 127.5, 120.7, 118.2, 105.1, 61.3, 49.6, 47.5, 14.3. MS (ESI) m/z : $[\text{M} + \text{H}]^+$ 389.29. HRMS m/z : $[\text{M} + \text{H}]^+$ calcd for $\text{C}_{17}\text{H}_{18}\text{BrN}_4\text{O}_2$, 389.0613; found, 389.0609; $[\text{M} + \text{Na}]^+$ calcd, 411.0433; found, 411.0425.

Ethyl 4-(3-(1H-imidazol-1-yl)propylamino)-6-bromoquinoline-3-carboxylate (17). Compound 1 (1 g, 3.18 mmol) was dissolved in 1,4-dioxane (5 mL) under N_2 atmosphere. To the reaction mixture, dry DIPEA (1.11 mL, 6.36 mmol) and 3-(1H-imidazol-1-yl)propan-1-amine (0.57 mL, 4.77 mmol) were added. The reaction mixture was allowed to stir for 12 h at room temperature. Then it was poured into 50 mL of water. The solid obtained was filtered and dried to give compound 17 as a white solid (1.2 g, 94% yield). ^1H NMR (600 MHz, CDCl_3): δ 9.29 (t, J = 4.8 Hz, -NH), 9.10 (s, 1H), 8.23 (d, J = 2.4 Hz, 1H), 7.82 (d, J = 9.0 Hz, 1H), 7.73 (dd, J = 9.0, 1.8 Hz, 1H), 7.46 (s, 1H), 7.06 (s, 1H), 6.90 (s, 1H), 4.41 (q, J = 7.2 Hz, 2H), 4.15 (t, J = 7.2 Hz, 2H), 3.78–3.75 (m, 2H), 2.28–2.23 (m, 2H), 1.43 (t, J = 7.2 Hz, 3H). ^{13}C NMR (150 MHz, CDCl_3): δ 168.9, 156.0, 151.8, 149.8, 137.1, 134.5, 131.7, 130.0, 128.0, 120.7, 118.7, 117.8, 103.8, 61.2, 45.3, 43.8, 32.4, 14.3. MS (ESI) m/z : $[\text{M} + \text{H}]^+$ 403.32. HRMS m/z : $[\text{M} + \text{H}]^+$ calcd for $\text{C}_{18}\text{H}_{20}\text{BrN}_4\text{O}_2$, 403.0769; found, 403.0787.

General Procedure D. 4-(2-(1H-imidazol-1-yl)ethylamino)-6-bromoquinoline-3-carbohydrazide (18). Compound 16 (1 g, 2.58 mmol) was dissolved in ethanol (10 mL). To the solution, hydrazine hydrate (10 mL) was added. The reaction mixture was stirred for 10 h at room temperature. Ethanol was removed under vacuum. The residue was dissolved in CHCl_3 , and the organic layer was washed with water and brine, dried, and concentrated to give compound 18 (0.82 g, 85% yield) as a yellow solid. mp > 250 °C. ^1H NMR (600 MHz, CD_3OD): δ 8.40 (s, 1H), 8.31 (d, J = 1.8 Hz, 1H), 7.78 (dd, J = 9.0, 1.8 Hz, 1H), 7.71 (d, J = 8.4 Hz, 1H), 7.59 (s, 1H), 7.09 (s, 1H), 6.91 (s, 1H), 4.31 (t, J = 6.0 Hz, 2H), 3.83 (t, J = 6.0 Hz, 2H), 1.81 (s, -CONHNH₂, 2H). ^{13}C NMR (150 MHz, CD_3OD): δ 168.6, 149.7, 149.2, 146.6, 137.3, 133.5, 129.8, 127.8, 124.8, 121.0, 119.4, 118.9, 109.0, 46.1, 46.0. MS (ESI) m/z : $[\text{M} + \text{H}]^+$ 375.05. HRMS m/z : $[\text{M} + \text{H}]^+$ calcd for $\text{C}_{15}\text{H}_{16}\text{BrN}_6\text{O}$, 375.0569; found, 375.0575.

4-(3-(1H-imidazol-1-yl)propylamino)-6-bromoquinoline-3-carbohydrazide (19). Compound 17 (1 g, 2.48 mmol) was dissolved in ethanol (10 mL). To the solution, hydrazine hydrate (10 mL) was added, and the reaction was performed according to general procedure D. The residue was dissolved in CHCl_3 , and the organic layer was washed with water and brine, dried, and concentrated to give compound 19 as a light green solid (0.75 g, 78% yield). mp > 250 °C. ^1H NMR (300 MHz, CD_3OD): δ 9.68 (br s, -NH), 8.59 (d, J = 1.2 Hz, 1H), 8.31 (s, 1H), 7.78 (dd, J = 8.7, 1.5 Hz, 1H), 7.72 (d, J = 8.7 Hz, 1H), 7.60 (s, 1H), 7.42 (t, J = 5.1 Hz, -CONH), 7.16 (s, 1H), 6.88 (s, 1H), 4.52 (br s, -CONHNH₂), 4.02 (t, J = 6.9 Hz, 2H), 3.32–3.26 (m, 2H), 2.10–2.01 (m, 2H). ^{13}C NMR (75 MHz, CD_3OD): δ 167.8, 150.5, 147.7, 147.0, 137.3, 132.6, 131.2, 128.4, 125.0, 121.0, 119.3, 117.7, 109.5, 43.8, 42.2, 30.8. MS (ESI) m/z : $[\text{M} + \text{H}]^+$ 389.28. HRMS m/z : $[\text{M} + \text{H}]^+$ calcd for $\text{C}_{16}\text{H}_{18}\text{BrN}_6\text{O}$, 389.0725; found, 389.0724.

General Procedure E. N-(2-(1H-imidazol-1-yl)ethyl)-6-bromo-3-(1,3,4-oxadiazol-2-yl)quinolin-4-amine (20). Compound 18 (1 g, 2.67 mmol) was taken in triethyl orthoformate (5 mL, 30.06 mmol), and the mixture was heated for 12 h at 100 °C. The residue was purified by column chromatography, eluting with 4% methanol in CHCl_3 to give compound 20 as a yellow solid (0.22 g, 43% yield). mp 197 °C. ^1H NMR (600 MHz, $\text{DMSO}-d_6$): δ 9.42 (s, 1H), 8.78 (s, 1H), 8.50 (d, J = 2.4 Hz, 1H), 8.14 (t, J = 5.4 Hz, -NH), 7.89 (dd, J = 9.0, 2.4 Hz, 1H), 7.82 (d, J = 9.0 Hz, 1H), 7.55 (s, 1H), 7.09 (s, 1H), 6.78 (s, 1H), 4.27 (t, J = 6.0 Hz, 2H), 3.86–3.84 (m, 2H). ^{13}C NMR (150 MHz, CDCl_3): δ 163.5, 151.4, 151.3, 149.1, 148.4, 137.5, 134.5, 132.1, 130.1, 127.2, 120.4, 119.0, 118.7, 100.7, 49.9, 47.5. MS (ESI) m/z : $[\text{M} + \text{H}]^+$ 385.27. HRMS m/z : $[\text{M} + \text{H}]^+$ calcd for $\text{C}_{16}\text{H}_{14}\text{BrN}_6\text{O}$, 385.0412; found, 385.0409.

N-(3-(1H-imidazol-1-yl)propyl)-6-bromo-3-(1,3,4-oxadiazol-2-yl)quinolin-4-amine (21). Compound 19 (1 g, 2.57 mmol) was taken in triethyl orthoformate (5 mL, 30.06 mmol), and the mixture was heated for 12 h at 110 °C. The reaction was carried out according to general procedure E. The crude mixture was purified by column chromatography, eluting with 3% methanol in CHCl_3 to afford compound 21 as a yellow solid (0.2 g, 19% yield). mp 147 °C. ^1H NMR (600 MHz, $\text{DMSO}-d_6$): δ 9.40 (s, 1H), 8.77 (s, 1H), 8.56 (d, J = 1.8 Hz, 1H), 8.18 (br s, -NH), 7.87 (dd, J = 9.0, 1.8 Hz, 1H), 7.81

(d, $J = 9.0$ Hz, 1H), 7.56 (s, 1H), 7.11 (s, 1H), 6.87 (s, 1H), 4.03 (t, $J = 7.2$ Hz, 2H), 3.43–3.40 (m, 2H), 2.13–2.08 (m, 2H). ^{13}C NMR (150 MHz, CDCl_3): δ 163.9, 151.4, 151.2, 149.2, 148.5, 134.5, 131.9, 127.8, 120.3, 118.5, 99.4, 45.7, 32.3, 29.7. MS (ESI) m/z : $[\text{M} + \text{H}]^+$ 399.37. HRMS m/z : $[\text{M} + \text{H}]^+$ calcd for $\text{C}_{17}\text{H}_{16}\text{BrN}_6\text{O}$, 399.0569; found, 399.0565. HPLC purity 97.38%.

General Procedure F. *N*-(2-(1*H*-imidazol-1-yl)ethyl)-6-(4-methoxyphenyl)-3-(1,3,4-oxadiazol-2-yl)quinolin-4-amine (**22**). Compound **20** (0.07 g, 0.18 mmol) was dissolved in a mixture of 1,4-dioxane (4 mL) and DMF (1 mL) under argon atmosphere. 2-(4-Methoxyphenyl)-4,4,5,5-tetramethyl-1,3,2-dioxaborolane (0.043 g, 0.18 mmol) was added to the mixture. 2(M) Na_2CO_3 solution (0.24 mL) was added to the reaction mixture, and argon was purged for 15 min. $\text{Pd}(\text{PPh}_3)_4$ (0.017 g, 0.014 mmol) was added to the mixture, and argon purging was performed for 15 min. The mixture was heated for 12 h at 100 °C. 1,4-Dioxane was removed under vacuum, the residue was dissolved in CHCl_3 , and the organic layer was washed with water and brine, dried, and concentrated. The residue was purified by silica gel column chromatography to afford compound **22** as a white solid (0.02 g, 27% yield). mp 213 °C. ^1H NMR (600 MHz, CDCl_3): δ 9.05 (s, 1H), 8.62 (t, $J = 4.2$ Hz, 1H), 8.52 (s, 1H), 8.21 (d, $J = 1.8$ Hz, 1H), 8.08 (d, $J = 9.0$ Hz, 1H), 7.95 (dd, $J = 9.0, 1.8$ Hz, 1H), 7.58 (d, $J = 8.4$ Hz, 2H), 7.46 (s, 1H), 7.06 (d, $J = 8.4$ Hz, 2H), 6.98 (s, 1H), 6.91 (s, 1H), 4.36–4.33 (m, 4H), 3.90 (s, 3H). ^{13}C NMR (150 MHz, CDCl_3): δ 163.8, 159.7, 152.6, 151.2, 149.4, 147.7, 138.0, 137.5, 132.6, 130.7, 130.1, 128.4, 122.2, 119.6, 118.7, 114.7, 100.7, 55.5, 50.1, 47.6. MS (ESI) m/z : $[\text{M} + \text{H}]^+$ 413.16. HRMS (ESI) m/z : $[\text{M} + \text{H}]^+$ calcd for $\text{C}_{23}\text{H}_{21}\text{N}_6\text{O}_2$, 413.1726; found, 413.1732. HPLC purity 98.37%.

N-(3-(1*H*-imidazol-1-yl)propyl)-3-(1,3,4-oxadiazol-2-yl)-6-phenylquinolin-4-amine (**23**). Compound **21** (0.08 g, 0.20 mmol) was taken along with phenylboronic acid (0.049 g, 0.40 mmol) in 1,4-dioxane (4 mL) and DMF (1 mL). 2(M) Na_2CO_3 solution (0.25 mL) and $\text{Pd}(\text{PPh}_3)_4$ (0.018 g, 0.016 mmol) were added to the mixture, and the reaction was performed according to procedure B. The residue was purified by silica gel column chromatography, eluting with 4% methanol in CHCl_3 to produce compound **23** as a white solid (0.032 g, 40% yield). mp 177 °C. ^1H NMR (300 MHz, CDCl_3): δ 9.11 (s, 1H), 8.82 (br s, –NH), 8.53 (s, 1H), 8.38 (s, 1H), 8.09 (d, $J = 9.0$ Hz, 1H), 7.98 (d, $J = 8.4$ Hz, 1H), 7.63 (d, $J = 7.5$ Hz, 2H), 7.53 (t, $J = 7.5$ Hz, 2H), 7.46–7.41 (m, 2H), 7.04 (s, 1H), 6.91 (s, 1H), 4.22 (t, $J = 6.9$ Hz, 2H), 4.03–3.98 (m, 2H), 2.41–2.32 (m, 2H). ^{13}C NMR (150 MHz, CDCl_3): δ 164.2, 152.7, 151.1, 149.9, 148.2, 140.4, 138.0, 137.1, 130.8, 130.7, 129.9, 129.2, 127.9, 127.3, 123.6, 119.3, 118.8, 99.2, 46.0, 44.0, 32.5. MS (ESI) m/z : $[\text{M} + \text{H}]^+$ 397.43. HRMS (ESI) m/z : $[\text{M} + \text{H}]^+$ calcd for $\text{C}_{23}\text{H}_{21}\text{N}_6\text{O}$, 397.1777; found, 397.1771. HPLC purity 99.53%.

4-(4-(3-(1*H*-imidazol-1-yl)propylamino)-3-(1,3,4-oxadiazol-2-yl)-quinolin-6-yl)benzonitrile (**24**). Compound **21** (0.08 g, 0.20 mmol) was taken along with 4-(4,4,5,5-tetramethyl-1,3,2-dioxaborolan-2-yl)benzonitrile (0.092 g, 0.40 mmol) in 1,4-dioxane (4 mL) and DMF (1 mL). 2(M) Na_2CO_3 solution (0.25 mL) and $\text{Pd}(\text{PPh}_3)_4$ (0.018 g, 0.016 mmol) were added to the mixture, and the reaction was performed according to procedure B. The residue was purified by silica gel column chromatography, eluting with 4% methanol in CHCl_3 to afford compound **24** as a bright yellow solid (0.035 g, 41% yield). mp 238 °C. ^1H NMR (300 MHz, $\text{CDCl}_3 + 1$ drop CD_3OD): δ 8.86 (s, 1H), 8.56 (s, 1H), 8.22 (s, 1H), 7.88 (d, $J = 8.7$ Hz, 1H), 7.78 (dd, $J = 8.7, 1.5$ Hz, 1H), 7.64 (d, $J = 8.4$ Hz, 2H), 7.56 (d, $J = 8.1$ Hz, 2H), 7.31 (s, 1H), 6.77 (d, $J = 4.8$ Hz, 2H), 4.06 (t, $J = 6.9$ Hz, 2H), 3.76 (m, 2H), 2.24–2.15 (m, 2H). ^{13}C NMR (150 MHz, CDCl_3): δ 164.1, 152.6, 151.2, 150.5, 148.8, 144.8, 137.2, 135.8, 133.0, 131.2, 130.2, 130.0, 127.9, 124.3, 119.4, 118.8, 118.7, 111.5, 99.5, 46.0, 43.9, 32.3. MS (ESI) m/z : $[\text{M} + \text{H}]^+$ 422.04. HRMS (ESI) m/z : $[\text{M}]^+$ calcd for $\text{C}_{24}\text{H}_{20}\text{N}_7\text{O}$, 422.1729; found, 422.1747. HPLC purity 96.02%.

N-(3-(1*H*-imidazol-1-yl)propyl)-6-(4-fluorophenyl)-3-(1,3,4-oxadiazol-2-yl)quinolin-4-amine (**25**). Compound **21** (0.08 g, 0.20 mmol) was taken along with 4-fluorophenylboronic acid (0.056 g, 0.40 mmol) in 1,4-dioxane (4 mL) and DMF (1 mL). 2(M) Na_2CO_3

solution (0.25 mL) and $\text{Pd}(\text{PPh}_3)_4$ (0.018 g, 0.016 mmol) were added to the mixture, and the reaction was performed according to procedure B. It took 8 h for the reaction to complete. The residue was purified by silica gel column chromatography, eluting with 4% methanol in CHCl_3 to produce compound **25** as a pale yellow solid (0.025 g, 30% yield). mp 218 °C. ^1H NMR (600 MHz, CDCl_3): δ 9.09 (s, 1H), 8.80 (t, $J = 4.8$ Hz, –NH), 8.53 (s, 1H), 8.29 (d, $J = 1.8$ Hz, 1H), 8.07 (d, $J = 9.0$ Hz, 1H), 7.90 (dd, $J = 9.0, 1.8$ Hz, 1H), 7.58–7.55 (m, 2H), 7.46 (s, 1H), 7.20 (t, $J = 9.0$ Hz, 2H), 7.03 (s, 1H), 6.89 (s, 1H), 4.22 (t, $J = 6.6$ Hz, 2H), 3.98–3.96 (m, 2H), 2.37–2.33 (m, 2H). ^{13}C NMR (150 MHz, CDCl_3): δ 164.2, 152.6, 151.1, 149.8, 148.2, 137.1, 137.0, 130.8, 130.6, 130.0, 128.9, 123.4, 119.4, 118.8, 116.2, 116.1, 99.3, 46.0, 43.9, 32.4. ESI-MS m/z : $[\text{M} + \text{H}]^+$ 415.16. HRMS (ESI) m/z : $[\text{M} + \text{H}]^+$ calcd for $\text{C}_{23}\text{H}_{20}\text{FN}_6\text{O}$, 415.1682; found, 415.1682. HPLC purity 96.60%.

4-(4-(3-(1*H*-imidazol-1-yl)propylamino)-3-(1,3,4-oxadiazol-2-yl)quinolin-6-yl)phenol (**26**). Compound **21** (0.10 g, 0.25 mmol) was taken along with 4-(4,4,5,5-tetramethyl-1,3,2-dioxaborolan-2-yl)phenol (0.11 g, 0.5 mmol) in 1,4-dioxane (4 mL) and DMF (1 mL). 2(M) Na_2CO_3 solution (0.3 mL) and $\text{Pd}(\text{PPh}_3)_4$ (0.023 g, 0.02 mmol) were added to the mixture, and the reaction was performed according to procedure B. After 7 h, the residue was purified by silica gel column chromatography, eluting with 10% methanol in CHCl_3 to get compound **26** as a pale yellow solid (0.04 g, 39% yield). mp > 250 °C. ^1H NMR (300 MHz, CD_3OD): δ 9.09 (s, 1H), 8.93 (s, 1H), 8.44 (d, $J = 1.5$ Hz, 1H), 8.02 (dd, $J = 8.7, 1.8$ Hz, 1H), 7.94 (d, $J = 8.7$ Hz, 1H), 7.65 (s, 1H), 7.57 (d, $J = 8.7$ Hz, 2H), 7.15 (s, 1H), 6.97 (s, 1H), 6.97–6.94 (m, 3H), 4.27 (t, $J = 6.9$ Hz, 2H), 3.98 (t, $J = 6.6$ Hz, 2H), 2.42–2.33 (m, 2H). ^{13}C NMR (150 MHz, $\text{CDCl}_3 + 1$ drop CD_3OD): δ 164.0, 157.3, 152.5, 151.3, 148.7, 147.4, 138.1, 136.9, 131.3, 130.7, 129.6, 129.3, 128.2, 122.5, 119.2, 118.9, 116.1, 99.0, 46.0, 44.4, 32.1. ESI-MS m/z : $(\text{M} + \text{H})^+$ 413.31. HRMS (ESI) m/z : $[\text{M} + \text{H}]^+$ calcd for $\text{C}_{23}\text{H}_{21}\text{N}_6\text{O}_2$, 413.1726; found, 413.1724. HPLC purity 99.09%.

N-(3-(1*H*-imidazol-1-yl)propyl)-3-(1,3,4-oxadiazol-2-yl)-6-*p*-tolylquinolin-4-amine (**27**). Compound **21** (0.07 g, 0.18 mmol) was taken along with *p*-tolylboronic acid (0.037 g, 0.27 mmol) in 1,4-dioxane (4 mL) and DMF (1 mL). 2(M) Na_2CO_3 solution (0.23 mL) and $\text{Pd}(\text{PPh}_3)_4$ (0.017 g, 0.014 mmol) were added to the mixture, and the reaction was performed according to procedure B. After 8 h, the residue was purified by silica gel column chromatography, eluting with 6% methanol in CHCl_3 to afford compound **27** as a yellow solid (0.037 g, 51% yield). mp 228 °C. ^1H NMR (600 MHz, CDCl_3): δ 9.07 (s, 1H), 8.77 (t, $J = 4.2$ Hz, –NH), 8.51 (s, 1H), 8.33 (d, $J = 1.8$ Hz, 1H), 8.05 (d, $J = 9.0$ Hz, 1H), 7.94 (dd, $J = 9.0, 1.8$ Hz, 1H), 7.51 (d, $J = 7.8$ Hz, 2H), 7.46 (s, 1H), 7.32 (d, $J = 7.8$ Hz, 2H), 7.04 (s, 1H), 6.90 (s, 1H), 4.21 (t, $J = 7.2$ Hz, 2H), 3.99–3.96 (m, 2H), 2.43 (s, 3H), 2.36–2.32 (m, 2H). ^{13}C NMR (150 MHz, CDCl_3): δ 164.2, 152.6, 151.0, 149.7, 148.0, 137.9, 137.4, 137.1, 130.7, 130.6, 129.9, 127.1, 123.2, 119.3, 118.8, 99.2, 46.0, 44.0, 32.5, 21.2. MS (ESI) m/z : $[\text{M} + \text{H}]^+$ 411.65. HRMS m/z : $[\text{M} + \text{H}]^+$ calcd for $\text{C}_{24}\text{H}_{23}\text{N}_6\text{O}$, 411.1933; found, 411.1930. HPLC purity 97.67%.

N-(3-(1*H*-imidazol-1-yl)propyl)-6-(4-methoxyphenyl)-3-(1,3,4-oxadiazol-2-yl)quinolin-4-amine (**28**). Compound **21** (0.10 g, 0.25 mmol) was taken along with 2-(4-methoxyphenyl)-4,4,5,5-tetramethyl-1,3,2-dioxaborolane (0.12 g, 0.5 mmol) in 1,4-dioxane (4 mL) and DMF (1 mL). 2(M) Na_2CO_3 solution (0.3 mL) and $\text{Pd}(\text{PPh}_3)_4$ (0.023 g, 0.02 mmol) were added to the reaction mixture, and the reaction was performed according to procedure B. The residue was purified by silica gel column chromatography, eluting with 7% methanol in CHCl_3 to afford compound **28** as a yellow solid (0.035 g, 33% yield). mp 202 °C. ^1H NMR (300 MHz, CD_3OD): δ 9.15 (s, 1H), 8.97 (s, 1H), 8.53 (s, 1H), 8.50 (s, 1H), 8.30 (d, $J = 8.7$ Hz, 1H), 7.98 (d, $J = 8.4$ Hz, 1H), 7.70 (d, $J = 8.7$ Hz, 2H), 7.50 (s, 1H), 7.32 (s, 1H), 7.10 (d, $J = 8.4$ Hz, 2H), 4.43 (t, $J = 7.2$ Hz, 2H), 4.13 (t, $J = 6.3$ Hz, 2H), 3.89 (s, 3H), 2.53–2.45 (m, 2H). ^{13}C NMR (75 MHz, CDCl_3): δ 164.2, 159.6, 152.6, 151.0, 149.4, 147.8, 137.6, 137.1, 132.8, 130.6, 130.5, 129.9, 128.3, 122.8, 119.4, 118.8, 114.6, 99.2, 55.4, 46.0, 44.0, 32.5. MS (ESI) m/z : $[\text{M} + \text{H}]^+$ 427.52. HRMS

(EI) m/z : $[M]^+$ calcd for $C_{24}H_{22}N_6O_2$, 426.1804; found, 426.1810. HPLC purity 98.44%.

N-(3-(1*H*-imidazol-1-yl)propyl)-6-(3-methoxyphenyl)-3-(1,3,4-oxadiazol-2-yl)quinolin-4-amine (**29**). Compound **21** (0.10 g, 0.25 mmol) was taken along with (3-methoxyphenyl)boronic acid (0.06 g, 0.38 mmol) in 1,4-dioxane (4 mL) and DMF (1 mL). 2(M) Na_2CO_3 solution (0.3 mL) and $Pd(PPh_3)_4$ (0.023 g, 0.02 mmol) were added to the reaction mixture, and the reaction was performed according to procedure B. The residue was purified by silica gel column chromatography, eluting with 9% methanol in $CHCl_3$ to get compound **29** as a pale yellow solid (0.052 g, 49% yield). mp 96 °C. 1H NMR (400 MHz, $CDCl_3$): δ 9.07 (s, 1H), 8.78 (t, J = 4.0 Hz, -NH), 8.50 (s, 1H), 8.34 (d, J = 2.0 Hz, 1H), 8.05 (d, J = 8.8 Hz, 1H), 7.93 (dd, J = 8.4, 2 Hz, 1H), 7.44 (d, J = 4.0 Hz, 1H), 7.41 (d, J = 8.0 Hz, 1H), 7.18 (dd, J = 7.6, 1.2 Hz, 1H), 7.14 (m, 1H), 7.01 (s, 1H), 6.94 (dd, J = 8.4, 1.6 Hz, 1H), 6.89 (s, 1H), 4.19 (t, J = 6.8 Hz, 2H), 3.99–3.95 (m, 2H), 3.88 (s, 3H), 2.37–2.30 (m, 2H). ^{13}C NMR (150 MHz, $CDCl_3$): δ 164.2, 160.2, 152.6, 151.1, 149.9, 148.2, 141.8, 137.8, 130.8, 130.6, 130.3, 129.9, 123.7, 119.7, 119.3, 118.9, 113.5, 112.7, 99.2, 55.4, 46.0, 44.0, 32.5. MS (ESI) m/z : $[M + H]^+$ 427.37. HRMS (ESI) m/z : $[M + H]^+$ calcd for $C_{24}H_{23}N_6O_2$, 427.1882; found, 427.1880. HPLC purity 95.44%.

N-(3-(1*H*-imidazol-1-yl)propyl)-6-(2-methoxyphenyl)-3-(1,3,4-oxadiazol-2-yl)quinolin-4-amine (**30**). Compound **21** (0.08 g, 0.2 mmol) was taken along with (2-methoxyphenyl)boronic acid (0.06 g, 0.4 mmol) in 1,4-dioxane (4 mL) and DMF (1 mL). 2(M) Na_2CO_3 solution (0.3 mL) and $Pd(PPh_3)_4$ (0.018 g, 0.02 mmol) were added to the reaction mixture, and the reaction was performed according to procedure B. The residue was purified by silica gel column chromatography, eluting with 8% methanol in $CHCl_3$ to get compound **30** as a white solid (0.024 g, 23% yield). mp 90 °C. 1H NMR (400 MHz, $CDCl_3$): δ 9.07 (s, 1H), 8.82 (br s, -NH), 8.50 (s, 1H), 8.39 (s, 1H), 8.03 (d, J = 6.6 Hz, 1H), 7.89 (d, J = 6.3 Hz, 1H), 7.44 (s, 1H), 7.39–7.35 (m, 2H), 7.09 (t, J = 5.4 Hz, 1H), 7.04–7.00 (m, 2H), 6.88 (s, 1H), 4.18 (t, J = 5.1 Hz, 2H), 3.97–3.93 (m, 2H), 3.80 (s, 3H), 2.33–2.30 (m, 2H). ^{13}C NMR (125 MHz, $CDCl_3$): δ 164.3, 156.5, 152.6, 151.0, 149.3, 147.9, 135.2, 133.3, 130.8, 129.6, 129.4, 126.1, 121.3, 118.7, 111.6, 98.8, 55.7, 45.7, 44.0, 32.5. MS (ESI) m/z : $[M + H]^+$ 427.29. HRMS (ESI) m/z : $[M + H]^+$ calcd for $C_{24}H_{23}N_6O_2$, 427.1882; found, 427.1889. HPLC purity 96.15%.

N-(3-(1*H*-imidazol-1-yl)propyl)-6-(3,4-dimethoxyphenyl)-3-(1,3,4-oxadiazol-2-yl)quinolin-4-amine (**31**). Compound **21** (0.10 g, 0.25 mmol) was taken along with 3,4-dimethoxyphenylboronic acid (0.091 g, 0.5 mmol) in 1,4-dioxane (4 mL) and DMF (1 mL). 2(M) Na_2CO_3 solution (0.3 mL) and $Pd(PPh_3)_4$ (0.023 g, 0.02 mmol) were added to the mixture, and the reaction was performed according to procedure B. After 24 h, the residue was purified by silica gel column chromatography, eluting with 7% methanol in $CHCl_3$ to afford compound **31** as an off-white solid (0.04 g, 35% yield). mp 205 °C. 1H NMR (300 MHz, $CDCl_3$): δ 9.09 (s, 1H), 8.72 (br s, -NH), 8.53 (s, 1H), 8.31 (s, 1H), 8.07 (d, J = 8.7 Hz, 1H), 7.94 (dd, J = 8.7, 1.2 Hz, 1H), 7.46 (s, 1H), 7.18–7.14 (m, 2H), 7.02 (d, J = 7.8 Hz, 2H), 6.90 (s, 1H), 4.22 (t, J = 6.9 Hz, 2H), 4.02–3.99 (m, 2H), 3.98 (s, 3H), 3.96 (s, 3H), 2.39–2.31 (m, 2H). ^{13}C NMR (75 MHz, $CDCl_3$): δ 164.2, 152.6, 151.0, 149.6, 149.5, 149.2, 148.0, 137.9, 137.1, 133.3, 130.7, 130.6, 129.9, 123.0, 119.7, 119.4, 118.8, 111.8, 110.6, 99.3, 56.1, 45.9, 43.9, 32.5. MS (ESI) m/z : $[M + H]^+$ 457.45. HRMS (ESI) m/z : $[M + H]^+$ calcd for $C_{25}H_{25}N_6O_3$, 457.1988; found, 457.1992. HPLC purity 95.37%.

N-(3-(1*H*-imidazol-1-yl)propyl)-6-(2,4-dimethoxyphenyl)-3-(1,3,4-oxadiazol-2-yl)quinolin-4-amine (**32**). Compound **21** (0.07 g, 0.18 mmol) was taken along with 2,4-dimethoxyphenylboronic acid (0.064 g, 0.36 mmol) in 1,4-dioxane (4 mL) and DMF (1 mL). 2(M) Na_2CO_3 solution (0.23 mL) and $Pd(PPh_3)_4$ (0.017 g, 0.014 mmol) were added to the mixture, and the reaction was performed according to procedure B. The crude product was purified by silica gel column chromatography, eluting with 7% methanol in $CHCl_3$ to afford compound **32** as a yellow solid (0.035 g, 44% yield). mp 140 °C. 1H NMR (300 MHz, $CDCl_3$): δ 9.07 (s, 1H), 8.80 (br s, -NH), 8.52 (s, 1H), 8.37 (d, J = 1.2 Hz, 1H), 8.02 (d, J = 8.4 Hz, 1H), 7.88 (dd, J =

9, 1.8 Hz, 1H), 7.47 (s, 1H), 7.30 (d, J = 8.4 Hz, 1H), 7.03 (s, 1H), 6.90 (s, 1H), 6.66–6.61 (m, 2H), 4.21 (t, J = 6.9 Hz, 2H), 4.00–3.93 (m, 2H), 3.89 (s, 3H), 3.80 (s, 3H), 2.37–2.28 (m, 2H). ^{13}C NMR (75 MHz, $CDCl_3$): δ 164.2, 160.8, 157.5, 152.5, 150.9, 149.1, 147.8, 134.9, 133.1, 131.2, 129.3, 125.6, 122.3, 118.7, 105.1, 99.2, 98.8, 55.6, 55.5, 45.6, 43.9, 32.4. MS (ESI) m/z : $[M + H]^+$ 457.51. HRMS (ESI) m/z : $[M + H]^+$ calcd for $C_{25}H_{25}N_6O_3$, 457.1988; found, 457.1985. HPLC purity 97.51%.

N-(3-(1*H*-imidazol-1-yl)propyl)-6-(4-methoxy-3-methylphenyl)-3-(1,3,4-oxadiazol-2-yl)quinolin-4-amine (**33**). Compound **21** (0.07 g, 0.18 mmol) was taken along with 4-methoxy-3-methylphenylboronic acid (0.058 g, 0.36 mmol) in 1,4-dioxane (4 mL) and DMF (1 mL). 2(M) Na_2CO_3 solution (0.23 mL) and $Pd(PPh_3)_4$ (0.017 g, 0.014 mmol) were added to the mixture, and the reaction was performed according to procedure B. The residue was purified by silica gel column chromatography, eluting with 7% methanol in $CHCl_3$ to produce compound **33** as a pale yellow solid (0.031 g, 40% yield). mp 191 °C. 1H NMR (300 MHz, $CDCl_3$): δ 9.07 (s, 1H), 8.75 (br s, -NH), 8.52 (s, 1H), 8.29 (s, 1H), 8.04 (d, J = 8.7 Hz, 1H), 7.93 (dd, J = 8.7, 1.2 Hz, 1H), 7.46 (s, 1H), 7.43–7.41 (m, 2H), 7.03 (s, 1H), 6.96 (d, J = 9.3 Hz, 1H), 6.90 (s, 1H), 4.21 (t, J = 6.9 Hz, 2H), 4.02–3.96 (m, 2H), 3.90 (s, 3H), 2.39–2.34 (m, 2H), 2.33 (s, 3H). ^{13}C NMR (150 MHz, $CDCl_3$): δ 164.3, 157.8, 152.6, 151.0, 149.5, 147.9, 137.9, 137.1, 132.4, 130.7, 130.5, 130.0, 129.5, 127.4, 125.6, 122.7, 119.4, 118.8, 110.4, 99.2, 55.5, 46.0, 44.0, 32.6, 16.6. MS (ESI) m/z : $[M + H]^+$ 441.41. HRMS (ESI) m/z : $[M + H]^+$ calcd for $C_{25}H_{25}N_6O_2$, 441.2039; found, 441.2038. HPLC purity 96.92%.

N-(3-(1*H*-imidazol-1-yl)propyl)-6-(4-methoxy-2-methylphenyl)-3-(1,3,4-oxadiazol-2-yl)quinolin-4-amine (**34**). Compound **21** (0.08 g, 0.20 mmol) was taken along with 4-methoxy-2-methylphenylboronic acid (0.067 g, 0.40 mmol) in 1,4-dioxane (4 mL) and DMF (1 mL). 2(M) Na_2CO_3 solution (0.30 mL) and $Pd(PPh_3)_4$ (0.018 g, 0.016 mmol) were added to the mixture, and the reaction was performed according to procedure B. After 7 h, the residue was purified by silica gel column chromatography, eluting with 6% methanol in $CHCl_3$ to produce compound **34** as a yellow gummy liquid (0.040 g, 45% yield). 1H NMR (600 MHz, $CDCl_3$): δ 9.07 (s, 1H), 8.76 (br s, -NH), 8.52 (d, J = 1.8 Hz, 1H), 8.06 (s, 1H), 8.00 (d, J = 7.2 Hz, 1H), 7.66 (d, J = 8.4 Hz, 1H), 7.41 (s, 1H), 7.17 (d, J = 6.6 Hz, 1H), 6.98 (s, 1H), 6.84–6.83 (m, 3H), 4.16 (t, J = 4.8 Hz, 2H), 3.88–3.87 (m, 2H), 3.84 (s, 3H), 2.28 (m, 2H), 2.26 (s, 3H). ^{13}C NMR (125 MHz, $CDCl_3$): δ 164.2, 159.6, 152.4, 151.1, 149.3, 148.0, 138.4, 137.1, 136.8, 133.5, 133.2, 131.0, 129.7, 129.6, 125.6, 118.9, 118.8, 116.0, 111.5, 99.0, 55.3, 45.8, 43.9, 32.4, 20.9. MS (ESI) m/z : $[M + H]^+$ 441.15. HRMS (ESI) m/z : $[M + H]^+$ calcd for $C_{25}H_{25}N_6O_2$, 441.2039; found, 441.2040. HPLC purity 96.32%.

5-(4-(3-(1*H*-imidazol-1-yl)propylamino)-6-bromoquinolin-3-yl)-1,3,4-oxadiazol-2-amine (**35**). Compound **19** (0.5 g, 1.28 mmol) was dissolved in methanol (5 mL), to which cyanogen bromide (0.163 g, 1.54 mmol) was added. The mixture was refluxed for 4 h. Excess solvent was evaporated, and the organic part was extracted with $CHCl_3$, washed with saturated $NaHCO_3$ solution, dried, and concentrated to give compound **35** (0.1 g, 19% yield). mp > 250 °C. 1H NMR (600 MHz, $DMSO-d_6$): δ 8.67 (s, 1H), 8.43 (s, 1H), 8.25 (t, J = 3.6 Hz, -NH), 7.81 (dd, J = 9.0, 1.8 Hz, 1H), 7.78 (d, J = 8.4 Hz, 1H), 7.55 (s, 1H), 7.12 (s, 1H), 6.86 (s, 1H), 4.06 (t, J = 7.2 Hz, 2H), 3.59–3.56 (m, 2H), 2.14–2.09 (m, 2H). ^{13}C NMR (150 MHz, $DMSO-d_6$): δ 163.4, 157.0, 149.5, 148.9, 148.1, 133.6, 132.5, 132.0, 128.9, 127.2, 124.2, 120.6, 117.9, 100.2, 45.0, 43.8, 32.1. MS (ESI) m/z : $[M + H]^+$ 414.23. HRMS m/z : $[M + H]^+$ calcd for $C_{17}H_{17}BrN_7O$, 414.0678; found, 414.0671.

5-(4-(3-(1*H*-imidazol-1-yl)propylamino)-6-(4-methoxyphenyl)-quinolin-3-yl)-1,3,4-oxadiazol-2-amine (**36**). Compound **35** (0.07 g, 0.17 mmol) was taken along with 2-(4-methoxyphenyl)-4,4,5,5-tetramethyl-1,3,2-dioxaborolane (0.08 g, 0.34 mmol) in 1,4-dioxane (4 mL) and DMF (1 mL). 2(M) Na_2CO_3 solution (0.3 mL) and $Pd(PPh_3)_4$ (0.016 g, 0.014 mmol) were added to the mixture, and the reaction was performed according to procedure B. The residue was purified by silica gel column chromatography, eluting with 6% methanol in $CHCl_3$ to produce compound **36** as a brown solid (0.017

g, 23% yield). mp 215 °C. ¹H NMR (600 MHz, DMSO-*d*₆): δ 8.72 (s, 1H), 8.49 (s, 1H), 8.09 (d, *J* = 8.4 Hz, 1H), 7.96 (d, *J* = 8.4 Hz, 1H), 7.77 (d, *J* = 8.4 Hz, 2H), 7.57 (s, 1H), 7.43–7.40 (m, 2H), 7.12 (d, *J* = 9.0 Hz, 2H), 4.26 (t, *J* = 7.2 Hz, 2H), 3.85 (s, 3H), 3.82–3.80 (m, 2H), 2.30–2.25 (m, 2H). ¹³C NMR (150 MHz, DMSO-*d*₆): δ 163.5, 159.8, 156.8, 137.2, 136.5, 132.1, 130.3, 128.8, 122.1, 121.5, 119.4, 115.1, 99.8, 55.8, 45.8, 45.1, 31.3. MS (ESI) *m/z*: [M + H]⁺ 442.29. HRMS (ESI) *m/z*: [M + H]⁺ calcd for C₂₄H₂₄N₇O₂, 442.1991; found, 442.1991. HPLC purity 97.91%.

N-(3-(1*H*-imidazol-1-yl)propyl)-6-bromo-3-(5-methyl-1,3,4-oxadiazol-2-yl)quinolin-4-amine (37). Compound 19 (1 g, 2.57 mmol) was dissolved in ethanol (5 mL), and to the solution, triethyl orthoacetate (5 mL, 27.27 mmol) was added. The reaction mixture was refluxed for 6 h. The residue was purified by column chromatography, eluting with 4% methanol in CHCl₃ to give 37 as a yellow gummy compound (0.25 g, 24% yield). mp 105 °C. ¹H NMR (600 MHz, DMSO-*d*₆): δ 8.71 (s, 1H), 8.50 (d, *J* = 1.8 Hz, 1H), 8.16 (t, *J* = 4.8 Hz, –NH), 7.84 (dd, *J* = 9.0, 1.8 Hz, 1H), 7.78 (d, *J* = 8.4 Hz, 1H), 7.53 (s, 1H), 7.10 (s, 1H), 6.85 (s, 1H), 4.04 (t, *J* = 7.2 Hz, 2H), 2.59 (s, 3H), 2.13–2.08 (m, 2H). ¹³C NMR (100 MHz, CDCl₃): δ 164.2, 162.4, 151.2, 149.1, 148.4, 134.2, 131.9, 127.7, 120.4, 118.4, 99.9, 45.7, 44.0, 32.4, 11.1. MS (ESI) *m/z*: [M + H]⁺ 413.24. HRMS (ESI) *m/z*: [M + H]⁺ calcd for C₁₈H₁₈BrN₆O, 413.0725; found, 413.0718.

N-(3-(1*H*-imidazol-1-yl)propyl)-6-(4-methoxyphenyl)-3-(5-methyl-1,3,4-oxadiazol-2-yl)quinolin-4-amine (38). Compound 37 (0.10 g, 0.24 mmol) was taken along with 2-(4-methoxyphenyl)-4,4,5,5-tetramethyl-1,3,2-dioxaborolane (0.11 g, 0.5 mmol) in 1,4-dioxane (4 mL) and DMF (1 mL). 2(M) Na₂CO₃ solution (0.3 mL) and Pd(PPh₃)₄ (0.023 g, 0.02 mmol) were added to the mixture, and the reaction was performed according to procedure B. It took 6 h to complete the reaction. The residue was purified by silica gel column chromatography, eluting with 4% methanol in CHCl₃ to afford compound 38 as a white solid (0.033 g, 31% yield). mp 224 °C. ¹H NMR (600 MHz, CDCl₃): δ 9.02 (s, 1H), 8.73 (t, *J* = 4.8 Hz, –NH), 8.29 (d, *J* = 1.8 Hz, 1H), 8.04 (d, *J* = 9.0 Hz, 1H), 7.91 (dd, *J* = 8.4, 1.8 Hz, 1H), 7.55 (d, *J* = 8.4 Hz, 2H), 7.45 (s, 1H), 7.04 (d, *J* = 8.4 Hz, 2H), 7.03 (s, 1H), 6.90 (s, 1H), 4.20 (t, *J* = 7.2 Hz, 2H), 3.97–3.93 (m, 2H), 3.88 (s, 3H), 2.69 (s, 3H), 2.34–2.30 (m, 2H). ¹³C NMR (150 MHz, CDCl₃): δ 164.4, 162.2, 159.6, 152.3, 149.4, 147.8, 137.5, 137.1, 132.9, 130.5, 130.3, 129.9, 128.3, 122.7, 119.5, 118.8, 114.6, 99.8, 55.5, 45.9, 44.0, 32.5, 11.1. MS (ESI) *m/z*: [M + H]⁺ 441.72. HRMS (ESI) *m/z*: [M + H]⁺ calcd for C₂₅H₂₅N₆O₂, 441.2039; found, 441.2140. HPLC purity 95.01%.

*Ethyl 4-((3-(1*H*-imidazol-1-yl)propyl)amino)-6-(4-methoxyphenyl)quinoline-3-carboxylate (39). Compound 17 (0.1 g, 0.25 mmol) was taken along with 2-(4-methoxyphenyl)-4,4,5,5-tetramethyl-1,3,2-dioxaborolane (0.12 g, 0.51 mmol) in 1,4-dioxane (5 mL). 2(M) Na₂CO₃ solution (0.3 mL) and Pd(PPh₃)₄ (0.023 g, 0.02 mmol) were added to the mixture, and the reaction was performed according to procedure B. The reaction was completed in 6 h. The residue was purified by silica gel column chromatography to afford compound 39 as a white solid (0.035 g, 33% yield). mp 190 °C. ¹H NMR (600 MHz, CD₃OD): δ 8.91 (s, 1H), 8.38 (s, 1H), 8.06 (d, *J* = 8.4 Hz, 1H), 7.87 (d, *J* = 8.4 Hz, 2H), 7.61 (d, *J* = 7.2 Hz, 2H), 7.24 (s, 1H), 7.07–7.06 (m, 3H), 4.42 (q, *J* = 7.2 Hz, 2H), 4.26 (t, *J* = 6.6 Hz, 2H), 3.95 (t, *J* = 6.6 Hz, 2H), 3.86 (s, 3H), 2.35–2.32 (m, 2H), 1.43 (t, *J* = 7.2 Hz, 3H). ¹³C NMR (150 MHz, CD₃OD): δ 167.7, 160.1, 157.2, 147.9, 138.1, 131.6, 128.0, 125.6, 123.1, 118.9, 114.3, 102.7, 61.3, 54.5, 48.2, 45.6, 31.2, 13.1. MS (ESI) *m/z*: [M + H]⁺ 431.08. HRMS (ESI) *m/z*: [M + H]⁺ calcd for C₂₅H₂₇N₄O₃, 431.2083; found, 431.2083. HPLC purity 98.92%.*

*Ethyl 4-((3-(1*H*-imidazol-1-yl)propyl)amino)-6-(3,4-dimethoxyphenyl)quinoline-3-carboxylate (40). Compound 17 (0.1 g, 0.25 mmol) was taken along with 3,4-dimethoxyphenylboronic acid (0.091 g, 0.5 mmol) in 1,4-dioxane (5 mL). 2(M) Na₂CO₃ solution (0.3 mL) and Pd(PPh₃)₄ (0.023 g, 0.02 mmol) were added to the mixture, and the reaction was performed according to procedure B. After 6 h, the residue was purified by silica gel column chromatography to get compound 40 as a white solid (0.038 g, 33%*

yield). mp 162 °C. ¹H NMR (300 MHz, CD₃OD): δ 8.98 (s, 1H), 8.54 (s, 1H), 8.24–8.22 (m, 2H), 7.95 (d, *J* = 8.7 Hz, 1H), 7.41 (s, 1H), 7.33–7.31 (m, 2H), 7.23 (s, 1H), 7.14 (d, *J* = 9.0 Hz, 1H), 4.48 (q, *J* = 6.9 Hz, 2H), 4.37 (t, *J* = 6.9 Hz, 2H), 4.13 (t, *J* = 6.3 Hz, 2H), 3.95 (s, 3H), 3.92 (s, 3H), 2.51–2.42 (m, 2H), 1.47 (t, *J* = 7.2 Hz, 3H). ¹³C NMR (150 MHz, CD₃OD): δ 167.0, 157.8, 149.9, 149.7, 145.9, 139.2, 132.9, 131.9, 123.7, 123.0, 120.4, 119.8, 118.5, 112.1, 110.8, 102.6, 61.8, 55.4, 55.1, 45.6, 45.1, 30.7, 13.1. MS (ESI) *m/z*: [M + H]⁺ 461.1117. HRMS (ESI) *m/z*: [M + H]⁺ calcd for C₂₆H₂₉N₄O₄, 461.2189; found, 461.2192. HPLC purity 98.80%.

*Ethyl 6-Bromo-4-(methylamino)quinoline-3-carboxylate (41). Compound 1 (0.5 g, 1.59 mmol) was dissolved in tetrahydrofuran (THF, 3 mL) under N₂ atmosphere in a sealed tube. To the reaction mixture, dry DIPEA (0.6 mL, 3.18 mmol) and methylamine (0.7 mL, 15.9 mmol) were added. The reaction mixture was heated for 16 h at 60 °C. Organic part was extracted with chloroform. The crude was purified by column chromatography to obtain compound 41 (0.2 g, 41% yield). mp 134 °C. ¹H NMR (300 MHz, CDCl₃): δ 9.48 (br s, –NH), 9.07 (s, 1H), 8.48 (d, *J* = 1.8 Hz, 1H), 7.81 (d, *J* = 9.0 Hz, 1H), 7.72 (dd, *J* = 8.7, 2.1 Hz, 1H), 4.38 (q, *J* = 7.2 Hz, 2H), 3.50 (d, *J* = 5.4 Hz, 3H), 1.42 (t, *J* = 7.2 Hz, 3H). ¹³C NMR (150 MHz, CDCl₃): δ 168.8, 156.4, 151.8, 149.8, 134.3, 131.5, 128.4, 120.5, 117.2, 102.8, 60.9, 35.4, 14.3. ESI-MS *m/z*: 309.02 [M + H]⁺. HRMS (ESI) *m/z*: [M + H]⁺ calcd for C₁₃H₁₄BrN₂O₂, 309.0238; found, 309.0236.*

*6-Bromo-4-(methylamino)quinoline-3-carbohydrazide (42). Compound 41 (0.5 g, 1.62 mmol) was dissolved in ethanol (8 mL). To the solution, hydrazine hydrate (8 mL) was added. The reaction mixture was stirred for 12 h at room temperature. Ethanol was removed under vacuum. The residue was then dissolved in CHCl₃, and the organic layer was washed with water and brine, dried, and concentrated to give compound 42 as a yellow solid (0.34 g, 73% yield). mp > 250 °C. ¹H NMR (600 MHz, DMSO-*d*₆): δ 9.59 (s, 1H), 8.51 (d, *J* = 1.8 Hz, 1H), 8.26 (s, –CONH–, 1H), 7.74 (dd, *J* = 9.0, 1.8 Hz, 1H), 7.69 (d, *J* = 9.0 Hz, 1H), 2.91 (d, *J* = 4.8 Hz, 3H). ¹³C NMR (100 MHz, CDCl₃ + 1 drop CD₃OD): δ 150.3, 149.9, 133.3, 129.6, 124.8, 118.5, 31.3. ESI-MS *m/z*: 295.24 (M + H)⁺. HRMS (ESI) *m/z*: [M + H]⁺ calcd for C₁₁H₁₂BrN₄O, 295.0194; found, 295.0192.*

*6-Bromo-N-methyl-3-(1,3,4-oxadiazol-2-yl)quinolin-4-amine (43). Compound 42 (0.5 g, 1.7 mmol) was taken in triethyl orthoformate (5 mL, 30.06 mmol), and the mixture was heated for 14 h at 140 °C. The residue was purified by column chromatography, eluting with 4% methanol in CHCl₃ to afford compound 43 as a yellow solid (0.15 g, 29% yield). mp 220 °C. ¹H NMR (300 MHz, CDCl₃): δ 9.02 (s, 1H), 8.57 (s, 1H), 8.48 (s, 1H), 7.86 (d, *J* = 9.0 Hz, 1H), 7.76 (dd, *J* = 9.0, 1.5 Hz, 1H), 3.62 (d, *J* = 5.1 Hz, 3H). ¹³C NMR (100 MHz, CDCl₃): δ 152.1, 151.0, 148.6, 134.2, 131.8, 128.2, 120.3, 117.9, 98.6, 35.7. ESI-MS *m/z*: 304.86 [M + H]⁺. HRMS (ESI) *m/z*: [M + H]⁺ calcd for C₁₂H₉BrN₄O, 305.0038; found, 305.0029.*

*6-(4-Methoxyphenyl)-N-methyl-3-(1,3,4-oxadiazol-2-yl)quinolin-4-amine (44). Compound 43 (0.1 g, 0.33 mmol) was taken along with 2-(4-methoxyphenyl)-4,4,5,5-tetramethyl-1,3,2-dioxaborolane (0.12 g, 0.51 mmol) in 1,4-dioxane (5 mL). 2(M) Na₂CO₃ solution (0.4 mL) and Pd(PPh₃)₄ (0.03 g, 0.03 mmol) were added to the mixture, and the reaction was performed according to procedure B. The residue was purified by silica gel column chromatography to afford compound 40 as a white solid (0.038 g, 35% yield). mp 155 °C. ¹H NMR (600 MHz, CDCl₃): δ 9.03 (s, –NH), 8.57 (s, 1H), 8.48 (s, 1H), 8.05 (d, *J* = 8.4 Hz, 1H), 7.93 (d, *J* = 8.4 Hz, 1H), 7.62 (d, *J* = 7.8 Hz, 2H), 7.05 (d, *J* = 7.8 Hz, 2H), 6.79 (s, 1H), 3.89 (s, 3H), 3.71 (d, *J* = 4.8 Hz, 3H). ¹³C NMR (150 MHz, CDCl₃): δ 164.2, 159.5, 153.2, 150.8, 147.9, 137.0, 133.0, 130.3, 130.2, 128.3, 123.3, 119.3, 116.1, 114.8, 114.6, 98.3, 55.5, 36.0. MS (ESI) *m/z*: [M + H]⁺ 333.55. HRMS *m/z*: [M + H]⁺ calcd for C₁₉H₁₇N₄O₂, 333.1351; found, 333.1338. HPLC purity 95.14%.*

Recombinant Human Top1 and Plasmid DNA Relaxation Assay. The recombinant human Top1 was purified from Sf-9 insect cells which were infected with the recombinant baculovirus (a kind gift from Prof. James J. Champoux) as described previously.^{12,20} The

type 1 DNA topoisomerases are assayed by the decreased mobility of the relaxed isomers of supercoiled pBS (SK+) DNA in 1% agarose gel. The relaxation assay was carried out with recombinant human Top1 or the whole cell extracts of MCF7 cells as a source of endogenous Top1, diluted in the relaxation buffer with supercoiled plasmid DNA as described previously.^{12,38,40}

Cleavage Assay. Plasmid DNA cleavage assay was carried out as described previously.^{12,20} Equilibrium cleavage assays with a 25-mer duplex of an oligonucleotide containing a Top1 binding motif were labeled and annealed as described previously.^{38,40} Samples were analyzed by 12% sequencing gel electrophoresis, dried, exposed on PhosphorImager screens, and imaged with Typhoon FLA 7000 (GE Healthcare, UK).

Analysis of Compound 28–DNA Intercalation. The ability of the drug to intercalate into plasmid DNA was determined by Top1 unwinding assay.^{12,40} Assays were performed with 50 fmol of pBluscript (SK+) DNA in the presence or absence of compound 28, *m*-AMSA, and etoposide. Relaxed DNA was prepared by treatment of the supercoiled plasmid DNA with an excess of Top1, followed by proteinase K digestion at 37 °C, phenol/chloroform extraction, and ethanol precipitation. After incubation at 37 °C for 15 min, reactions were terminated and electrophoresed onto 1% agarose gel as described above. The DNA band was stained with 0.5 $\mu\text{g/mL}$ of EtBr and visualized by UV light as described above.

Second, an ethidium displacement fluorescence assay⁴⁰ was employed to determine whether compound 28 binds in the minor groove of DNA. Fluorescence emission spectra ($\lambda_{\text{max}} = 590 \text{ nm}$, excitation wavelength 510 nm) were obtained at 25 °C. The assays contained 1 μM EtBr, 0–300 mM compound 28, and 5 nM CT DNA in 2 mL of fluorescence buffer.

Cell Culture and Transfection. Human cancerous cell lines such as MCF7, HeLa, HCT116, NIH: OVCAR-3, and HEK293 obtained from the Developmental Therapeutics Program as a kind gift from Dr. Yves Pommier (NIH/NCI/USA) and TDP1+/+ and TDP1–/– primary MEF (mouse embryonic fibroblasts) cells as a kind gift from Dr. Cornelius F. Boerkoel (University of British Columbia, Canada) were cultured as described previously.^{51,53} Plasmid DNAs were transfected with Lipofectamine 2000 (Invitrogen) according to the manufacturer's protocol.

Photobleaching Experiments. Photobleaching experiments were performed as described previously^{12,51} using an Andor Spinning disk inverted confocal laser-scanning microscope equipped with a 60 \times /1.42 NA oil-immersion objective (Olympus) and with a CO₂-controlled on-stage heated environmental chamber set to 37 °C. FRAP analyses were carried out with living MCF7 cells that ectopically express EGFP-human Top1 constructs (wild-type and N722S),⁵⁰ which were grown on chamber cover glass (Genetix, India) and drug-treated as indicated. For FRAP analysis, a subnuclear spot was bleached for 30 ms by solid-state laser line (488 nm for EGFP) adapted to the fluorescent protein of interest, and FRAP curves were generated individually normalized to the prebleach signal as described previously.^{50,52,53}

Immunocytochemistry and Confocal Microscopy. Immunofluorescence staining and confocal microscopy were performed as described previously.^{51–53} After treatment, MCF7 cells were fixed with 4% paraformaldehyde for 10 min at room temperature. Primary antibody against γH2AX (Cell Signaling, USA) was detected using anti-mouse IgG secondary antibodies labeled with Alexa 488 (Invitrogen). Cells were mounted in anti-fade solution with 4',6-diamidino-2-phenylindole (Vector Laboratories, Burlingame, CA) and examined using a laser scanning confocal microscope (Leica TCS SP8 confocal laser-scanning microscope) with a $\times 63$ oil objective. The γH2AX intensity per nucleus was determined with Adobe Photoshop 7.0 by measuring the fluorescence intensities normalized to the number of cell count.⁵¹

Cell Survival Assay. Cell survival was assessed by the 3-(4,5-dimethylthiazol-2-yl)-2,5-diphenyltetrazolium bromide assay as discussed previously.^{12,20} The percent inhibition of viability for each concentration of the compounds was calculated with respect to the control, and IC₅₀ values were estimated.

Molecular Docking Study. The molecular docking experiment was performed for selected compounds with LibDock in Discovery Studio 4.1 client. The ligand centroid coordinates of the ternary complex for docking were defined using the ligand in the Top1–DNA–CPT crystal structure (PDB code 1T8I) as the center of the binding pocket ($x = 21.386168$, $y = -2.148207$, $z = 28.116527$). The docking study suggests the probable binding poses of these inhibitors in the binding site in the Top1–DNA cleavage complex. The best poses for every ligand were selected based on the hydrogen bond interaction with Arg364, Asn722, and Asp533 and π – π hydrophobic interactions. The entire complex was subsequently subjected to minimization using a full minimization method executing 2000 steps, which maintained the root-mean-square gradient of 0.01 kcal mol^{–1}. The best binding pose of compound 28 is depicted in Figure 1D.

Aqueous Solubility Assay. Five microliters of 20 mM dimethyl sulfoxide (DMSO) stock from the stock plate was added to the reaction deep well plate containing 495 μL of pH 7.4 pION buffer, which includes DMSO control, and the samples were mixed and incubated for 18 h. The plate was sealed well during the incubation process. The DMSO content in the sample was <1.0%. The concentration in deep well plates was 200 μM . The working stock plate was prepared by adding 4 μL of 20 mM stock (including DMSO control) to 996 μL of acetonitrile. The working stock (75 μL) was added to 75 μL of blank buffer and read on a spectrophotometer as a reference plate at 240 nm. At the end of the incubation period, a filter plate was used to vacuum-filter 100 μL of the sample from the storage plate. This step wets the filters, and the filtrate was discarded. Another 200 μL of the sample from a deep well plate was vacuum-filtered into a new filter collection plate. The filtrate (75 μL) from the filter collection plate was transferred to a UV sample plate. Acetonitrile (75 μL) was added to this UV plate. The solution was mixed, and the spectrum was read using the UV spectrophotometer at 240 nm. Plates were read on spectramax using SoftMax Pro software version 5.3.

Human Plasma Stability Assay. The stock solution of 10 mM in DMSO was prepared and stored at 4 °C. Stock (25 μM) of the test compound was prepared in acetonitrile: water by diluting from the previously prepared 10 mM stock (i.e., 2.5 μL of 10 mM stock solution was added to 997.5 μL of acetonitrile/water (50:50). The frozen plasma was thawed at room temperature and centrifuged at 1400 \times RCF 4 °C, for 15 min. Approximately 90% of the clear supernatant fraction was transferred to a separate tube and was then used for the assay.

For 0 min samples, plasma was heat-inactivated at 56 °C for 45 min. Three microliters of 25 μM test compound was added to 72 μL of heat-inactivated plasma. A 25 μL aliquot of the mixture was taken and crashed with 200 μL of acetonitrile containing internal standard and further processed along with other time points. A final working stock of 1 μM was prepared by diluting in plasma for other time point samples (i.e., 8 μL of 25 μM acetonitrile/water stock was added to 192 μL of plasma). Two hundred microliters of plasma containing the test compound was incubated for 2 h at 37 °C in a shaker water bath with gentle shaking. A 25 μL aliquot of the sample at 0, 15, 30, 60, and 120 min was precipitated immediately with 200 μL of acetonitrile containing internal standard and centrifuged at 4000 \times RCF, 4 °C for 20 min. The supernatant (150 μL) was diluted with 150 μL of water and analyzed on liquid chromatography–mass spectrometry (LC–MS)/MS.

Lipophilicity Assay. NaH₂PO₄·2H₂O (1.56 g) was dissolved in 0.5 L of water in a 1 L beaker. The volume of the solution was made up to 1 L after adjusting the pH to 7.4 using NaOH solution. Equal volumes of sodium phosphate buffer (10 mM, pH 7.4) and *n*-octanol were added to a separation funnel and mixed thoroughly. The two layers were allowed to separate for 2 days and then dispensed in two separate glass bottles. Stock solution (10 mM) was prepared in 100% DMSO and stored at 4 °C. The organic phase (1-octanol) (500 μL) was added to each well of a 2 mL deep well plate, followed by 500 μL of buffer, and 15 μL of the test substance was added. The plate was vortexed for 1 h on a plate shaker at 1200 rpm. The samples were allowed to equilibrate for 20 min after incubation, centrifuged at 4000

rpm for 30 min for complete phase separation, and then analyzed by LC-UV.

Caco-2 Permeability Assay. Five microliters of 100 mM sodium pyruvate, 5 mL of 100× nonessential amino acids, and 5 mL of pen-strep were added to 100 mL of heat-inactivated fetal bovine serum to 385 mL of Dulbecco's modified Eagle's medium (DMEM) aseptically and mixed thoroughly. One vial of Hank's balanced salt (Sigma-H1387) was dissolved in 900 mL of Milli-Q water, and the pH was adjusted to 7.4. The volume was made up to 1000 mL with the same. The solution was filter-sterilized and stored at 4 °C. Stock solution of test compound (10 mM) was prepared in DMSO. Stock (10 mM) was diluted with Hank's balanced salt solution (HBSS) buffer to a final concentration of 10 μ M.

Revival of Caco-2 cells: as per SOP-BIO-IA-TCL-013-00.

Subculturing of Caco-2 cells: as per SOP-BIO-TCL-013-00.

DMEM (250 μ L) was added to the basal compartment of a 96-well multiscreen Caco-2 plate, 12 000 cells/well (0.16×10^6 cells/mL) were seeded in all the apical wells required and one well with only media as blank without cells, and the Caco-2 plate was placed in a CO₂ incubator at 37 °C for proliferation of cells. On the day of assay, the medium was removed and washed twice with HBSS buffer. The medium was incubated with HBSS buffer for 30 min in an incubator, and wells with transepithelial electrical resistance values $>230 \Omega \cdot \text{cm}^2$ were selected for the incubation. The test compound (75 μ L) was added to apical wells, and 250 μ L of HBSS buffer with 2% bovine serum albumin (BSA) was added to basal wells. Basal samples (25 μ L) were collected at 120 min and processed as mentioned below. The test compound (250 μ L) was added to basal wells, and 75 μ L of HBSS buffer with 2% BSA was added to apical wells. Apical samples (25 μ L) were collected at 120 min and processed as stated below. Single point calibration curve in HBSS buffer with 2% BSA was used. Donor samples were diluted 1:1 with HBSS containing 2% BSA, and receiver samples were diluted with 1.1 HBSS buffer. It was precipitated with 200 μ L of acetonitrile containing internal standard, vortexed for 5 min @ 1000 rpm, and then centrifuged at 4000 rpm for 10 min. Finally, 100 μ L of the supernatant was diluted with 200 μ L of water and submitted for LC-MS/MS analysis.

■ ASSOCIATED CONTENT

■ Supporting Information

The Supporting Information is available free of charge on the ACS Publications website at DOI: 10.1021/acs.jmedchem.8b01938.

X-ray crystal data of compound **28**, cytotoxicity data of compound **28** and CPT in various cell lines, molecular docking analysis of compounds **22**, **27**, **31**, and **33**, ¹H NMR and ¹³C NMR spectra of compounds **1–44**, and HPLC chromatogram of tested compounds (PDF)
Molecular formula strings (CSV)

■ AUTHOR INFORMATION

Corresponding Authors

*E-mail: pcbbd@iacs.res.in (B.B.D.).

*E-mail: atalukdar@iicb.res.in (A.T.).

ORCID

Benu Brata Das: 0000-0003-2519-7105

Arindam Talukdar: 0000-0002-7831-1795

Author Contributions

^{||}B.K., S.K.D., and S.P.C. equally contributed for this paper.

Notes

The authors declare no competing financial interest.

■ ACKNOWLEDGMENTS

The A.T. team would like to thank CSIR-IICB intramural research fund and DBT BT/Indo-Aus/10/22/2016 for

funding. B.K., S.P.C., and A.M. thank UGC for their fellowship. S.K.D. thanks IACS for SRF. S.P. would like to thank ICMR for SRF. D.S. and D.B. would like to thank DST-INSPIRE for fellowship. The B.B.D. team is supported by Wellcome Trust/DBT India Alliance intermediate fellowship grant (award# IA/I/13/1/500888) and IACS intramural funding. A.G. is an India Alliance SRF. B.B.D. is a Wellcome Trust/DBT India Alliance Intermediate fellow.

■ ABBREVIATIONS

HTop1, human topoisomerase 1; CPT, camptothecin; Top1cc, topoisomerase 1–DNA cleavage complexes; IC₅₀, the half-maximal inhibitory concentration; FRAP, fluorescence recovery after photobleaching; Pgp, permeability glycoprotein; ADME, absorption, distribution, metabolism, and excretion; DSBs, DNA double-strand breaks; DIPEA, *N,N*-diisopropylethylamine; pBS (SK+) DNA, pBluescript plasmid DNA; EGFP, enhanced green fluorescent protein

■ REFERENCES

- (1) Champoux, J. J. DNA topoisomerases: structure, function, and mechanism. *Annu. Rev. Biochem.* **2001**, *70*, 369–413.
- (2) Pommier, Y. Topoisomerase I inhibitors: camptothecins and beyond. *Nat. Rev. Cancer* **2006**, *6*, 789–802.
- (3) Wang, J. C. Cellular roles of DNA topoisomerases: a molecular perspective. *Nat. Rev. Mol. Cell Biol.* **2002**, *3*, 430–440.
- (4) Bansal, S.; Bajaj, P.; Pandey, S.; Tandon, V. Topoisomerases: resistance versus sensitivity, how far we can go? *Med. Res. Rev.* **2017**, *37*, 404–438.
- (5) Pommier, Y.; Marchand, C. Interfacial inhibitors: targeting macromolecular complexes. *Nat. Rev. Drug Discovery* **2011**, *11*, 25–36.
- (6) Pommier, Y. Drugging topoisomerases: lessons and challenges. *ACS Chem. Biol.* **2013**, *8*, 82–95.
- (7) Ghilarov, D. A.; Shkundina, I. S. DNA topoisomerases and their functions in a cell. *Mol. Biol.* **2012**, *46*, 47–57.
- (8) Kathiravan, M. K.; Khilare, M. M.; Nikoomanesh, K.; Chothe, A. S.; Jain, K. S. Topoisomerase as Target for Antibacterial and Anticancer Drug Discovery. *J. Enzyme Inhib. Med. Chem.* **2013**, *28*, 419–435.
- (9) Capranico, G.; Marinello, J.; Chillemi, G. Type I DNA topoisomerases. *J. Med. Chem.* **2017**, *60*, 2169–2192.
- (10) Akerman, K. J.; Fagenson, A. M.; Cyril, V.; Taylor, M.; Muller, M. T.; Akerman, M. P.; Munro, O. Q. Gold(III) macrocycles: nucleotide-specific unconventional catalytic inhibitors of human topoisomerase I. *J. Am. Chem. Soc.* **2014**, *136*, 5670–5682.
- (11) Cagir, A.; Jones, S. H.; Gao, R.; Eisenhauer, B. M.; Hecht, S. M.; Luotonen, A. Luotonen A. A Naturally Occurring Human DNA Topoisomerase I Poison. *J. Am. Chem. Soc.* **2003**, *125*, 13628–13629.
- (12) Das, S. K.; Ghosh, A.; Paul Chowdhuri, S.; Halder, N.; Rehman, I.; Sengupta, S.; Sahoo, K. C.; Rath, H.; Das, B. B. Neutral porphyrin derivative exerts anticancer activity by targeting cellular topoisomerase I (top1) and promotes apoptotic cell death without stabilizing top1-DNA cleavage complexes. *J. Med. Chem.* **2018**, *61*, 804–817.
- (13) Beretta, G. L.; Ribaud, G.; Menegazzo, I.; Supino, R.; Capranico, G.; Zunino, F.; Zagotto, G. Synthesis and evaluation of new naphthalene and naphthoquinone derivatives as anticancer agents. *Arch. Pharm.* **2017**, *350*, No. e1600286.
- (14) Pommier, Y. DNA topoisomerase I inhibitors: chemistry, biology, and interfacial inhibition. *Chem. Rev.* **2009**, *109*, 2894–2902.
- (15) Pommier, Y.; Cushman, M. The indenoisoquinoline non-camptothecin topoisomerase I inhibitors: update and perspectives. *Mol. Cancer Ther.* **2009**, *8*, 1008–1014.
- (16) Wall, M. E.; Wani, M. C.; Cook, C. E.; Palmer, K. H.; McPhail, A. T.; Sim, G. A. Plant Antitumor Agents. I. The Isolation and Structure of Camptothecin, a Novel Alkaloidal Leukemia and Tumor

Inhibitor from Camptotheca acuminata^{1,2}. *J. Am. Chem. Soc.* **1966**, *88*, 3888–3890.

(17) Strumberg, D.; Pommier, Y.; Paull, K.; Jayaraman, M.; Nagafuji, P.; Cushman, M. Synthesis of cytotoxic indenoisoquinoline topoisomerase I poisons. *J. Med. Chem.* **1999**, *42*, 446–457.

(18) Beck, D. E.; Agama, K.; Marchand, C.; Chergui, A.; Pommier, Y.; Cushman, M. Synthesis and biological evaluation of new carbohydrate-substituted indenoisoquinoline topoisomerase I inhibitors and improved syntheses of the experimental anticancer agents indotecan (LMP400) and indimitecan (LMP776). *J. Med. Chem.* **2014**, *57*, 1495–1512.

(19) Prudhomme, M. Biological targets of antitumor indolocarbazoles bearing a sugar moiety. *Curr. Med. Chem.: Anti-Cancer Agents* **2004**, *4*, 509–521.

(20) Majumdar, P.; Bathula, C.; Basu, S. M.; Das, S. K.; Agarwal, R.; Hati, S.; Singh, A.; Sen, S.; Das, B. B. Design, Synthesis and evaluation of thiohydantoin derivatives as potent topoisomerase I (top1) inhibitors with anticancer activity. *Eur. J. Med. Chem.* **2015**, *102*, 540–551.

(21) Beretta, G. L.; Zuco, V.; Perego, P.; Zaffaroni, N. Targeting DNA topoisomerase I with non-camptothecin poisons. *Curr. Med. Chem.* **2012**, *19*, 1238–1257.

(22) Pommier, Y.; Cushman, M.; Doroshow, J. H. Novel clinical indenoisoquinoline topoisomerase I inhibitors: a twist around the camptothecins. *Oncotarget* **2018**, *9*, 26466–26490.

(23) A phase I study of indenoisoquinolines LMP400 and LMP776 in adults with relapsed solid tumors and lymphomas. <https://clinicaltrials.gov/ct2/show/NCT01051635> (accessed Nov 1, 2018).

(24) Prijovich, Z. M.; Burnouf, P.-A.; Chou, H.-C.; Huang, P.-T.; Chen, K.-C.; Cheng, T.-L.; Leu, Y.-L.; Roffler, S. R. Synthesis and antitumor properties of BQC-Glucuronide, a camptothecin prodrug for selective tumor activation. *Mol. Pharm.* **2016**, *13*, 1242–1250.

(25) Xiao, X.; Antony, S.; Kohlhagen, G.; Pommier, Y.; Cushman, M. Novel autoxidative cleavage reaction of 9-fluoredenes discovered during synthesis of a potential DNA-threading indenoisoquinoline. *J. Org. Chem.* **2004**, *69*, 7495–7501.

(26) Morrell, A.; Antony, S.; Kohlhagen, G.; Pommier, Y.; Cushman, M. A systematic study of nitrated indenoisoquinolines reveals a potent topoisomerase I inhibitor. *J. Med. Chem.* **2006**, *49*, 7740–7753.

(27) Nagarajan, M.; Morrell, A.; Fort, B. C.; Meckley, M. R.; Antony, S.; Kohlhagen, G.; Pommier, Y.; Cushman, M. Synthesis and anticancer activity of simplified indenoisoquinoline topoisomerase I inhibitors lacking substituents on the aromatic rings. *J. Med. Chem.* **2004**, *47*, 5651–5661.

(28) Lv, P.-C.; Elsayed, M. S. A.; Agama, K.; Marchand, C.; Pommier, Y.; Cushman, M. Design, synthesis, and biological evaluation of potential prodrugs related to the experimental anticancer agent indotecan (LMP400). *J. Med. Chem.* **2016**, *59*, 4890–4899.

(29) Beck, D. E.; Reddy, P. V. N.; Lv, W.; Abdelmalak, M.; Tender, G. S.; Lopez, S.; Agama, K.; Marchand, C.; Pommier, Y.; Cushman, M. Investigation of the Structure-Activity Relationships of Aza-A-Ring Indenoisoquinoline Topoisomerase I Poisons. *J. Med. Chem.* **2016**, *59*, 3840–3853.

(30) Rasheed, Z. A.; Rubin, E. H. Mechanisms of resistance to topoisomerase I-targeting drugs. *Oncogene* **2003**, *22*, 7296–7304.

(31) Sirikantaramas, S.; Yamazaki, M.; Saito, K. Mutations in topoisomerase I as a self-resistance mechanism coevolved with the production of the anticancer alkaloid camptothecin in plants. *Proc. Natl. Acad. Sci. U.S.A.* **2008**, *105*, 6782–6786.

(32) Taliani, S.; Pugliesi, I.; Barresi, E.; Salerno, S.; Marchand, C.; Agama, K.; Simorini, F.; La Motta, C.; Marini, A. M.; Di Leva, F. S.; Marinelli, L.; Cosconati, S.; Novellino, E.; Pommier, Y.; Di Santo, R.; Da Settimo, F. Phenylpyrazolo[1,5-a]quinazolin-5(4H)-one: A suitable scaffold for the development of noncamptothecin topoisomerase I (top1) inhibitors. *J. Med. Chem.* **2013**, *56*, 7458–7462.

(33) Nagarajan, M.; Xiao, X.; Antony, S.; Kohlhagen, G.; Pommier, Y.; Cushman, M. Design, synthesis, and biological evaluation of indenoisoquinoline topoisomerase I inhibitors featuring polyamine

side chains on the lactam nitrogen. *J. Med. Chem.* **2003**, *46*, 5712–5724.

(34) Nagarajan, M.; Morrell, A.; Ioanoviciu, A.; Antony, S.; Kohlhagen, G.; Agama, K.; Hollingshead, M.; Pommier, Y.; Cushman, M. Synthesis and evaluation of indenoisoquinoline topoisomerase I inhibitors substituted with nitrogen heterocycles. *J. Med. Chem.* **2006**, *49*, 6283–6289.

(35) Cushman, M.; Jayaraman, M.; Vroman, J. A.; Fukunaga, A. K.; Fox, B. M.; Kohlhagen, G.; Strumberg, D.; Pommier, Y. Synthesis of New Indeno[1,2-c]isoquinolines: Cytotoxic Non-Camptothecin Topoisomerase I Inhibitors. *J. Med. Chem.* **2000**, *43*, 3688–3698.

(36) Fox, B. M.; Xiao, X.; Antony, S.; Kohlhagen, G.; Pommier, Y.; Staker, B. L.; Stewart, L.; Cushman, M. Design, Synthesis, and Biological Evaluation of Cytotoxic 11-Alkenylindenoisoquinoline Topoisomerase I Inhibitors and Indenoisoquinoline–Camptothecin Hybrids. *J. Med. Chem.* **2003**, *46*, 3275–3282.

(37) Cinelli, M. A.; Reddy, P. V. N.; Lv, P.-C.; Liang, J.-H.; Chen, L.; Agama, K.; Pommier, Y.; van Breemen, R. B.; Cushman, M. Identification, synthesis, and biological evaluation of metabolites of the experimental cancer treatment drugs indotecan (LMP400) and indimitecan (LMP776) and investigation of isomerically hydroxylated indenoisoquinoline analogues as topoisomerase I Poisons. *J. Med. Chem.* **2012**, *55*, 10844–10862.

(38) Das, B. B.; Sen, N.; Ganguly, A.; Majumder, H. K. Reconstitution and functional characterization of the unusual bi-subunit type I DNA topoisomerase from *Leishmania donovani*. *FEBS Lett* **2004**, *565*, 81–88.

(39) Das, B. B.; Sen, N.; Dasgupta, S. B.; Ganguly, A.; Majumder, H. K. N-terminal Region of the Large Subunit of *Leishmania donovani* Bi-subunit Topoisomerase I Is Involved in DNA Relaxation and Interaction with the Smaller Subunit. *J. Biol. Chem.* **2005**, *280*, 16335–16344.

(40) Das, B. B.; Sen, N.; Roy, A.; Dasgupta, S. B.; Ganguly, A.; Mohanta, B. C.; Dinda, B.; Majumder, H. K. Differential induction of *Leishmania donovani* bi-subunit topoisomerase I-DNA cleavage complex by selected flavones and camptothecin: activity of flavones against camptothecin-resistant topoisomerase I. *Nucleic Acids Res.* **2006**, *34*, 1121–1132.

(41) Staker, B. L.; Feese, M. D.; Cushman, M.; Pommier, Y.; Zembower, D.; Stewart, L.; Burgin, A. B. Structures of Three Classes of Anticancer Agents Bound to the Human Topoisomerase I–DNA Covalent Complex. *J. Med. Chem.* **2005**, *48*, 2336–2345.

(42) Pommier, Y.; Jenkins, J.; Kohlhagen, G.; Leteurtre, F. DNA recombinase activity of eukaryotic DNA topoisomerase I; effects of camptothecin and other inhibitors. *Mutat. Res., DNA Repair* **1995**, *337*, 135–145.

(43) Leeson, P. D.; Springthorpe, B. The influence of drug-like concepts on decision-making in medicinal chemistry. *Nat. Rev. Drug Discovery* **2007**, *6*, 881–890.

(44) Veber, D. F.; Johnson, S. R.; Cheng, H. Y.; Smith, B. R.; Ward, K. W.; Kopple, K. D. Molecular properties that influence the oral bioavailability of drug candidates. *J. Med. Chem.* **2002**, *45*, 2615–2623.

(45) Navia, M.; Chaturvedi, P. Design principles for orally bioavailable drugs. *Drug Discovery Today* **1996**, *1*, 179–189.

(46) Derakhshandeh, K.; Hochhaus, G.; Dadashzadeh, S. In-vitro Cellular Uptake and Transport Study of 9-Nitrocampothecin PLGA Nanoparticles Across Caco-2 Cell Monolayer Model. *Iran J. Pharm. Res.* **2011**, *10*, 425–434.

(47) Lalloo, A. K.; Luo, F. R.; Guo, A.; Paranjpe, P. V.; Lee, S.-H.; Vyas, V.; Rubin, E.; Sinko, P. J. Membrane transport of camptothecin: facilitation by human P-glycoprotein (ABCB1) and multidrug resistance protein 2 (ABCC2). *BMC Med.* **2004**, *2*, 16.

(48) Garcia-Carbonero, R.; Supko, J. G. Current perspectives on the clinical experience, pharmacology, and continued development of the camptothecins. *Clin. Cancer Res.* **2002**, *8*, 641–661.

(49) Slatter, J. G.; Schaaf, L. J.; Sams, J. P.; Feenstra, K. L.; Johnson, M. G.; Bombardt, P. A.; Cathcart, K. S.; Verburg, M. T.; Pearson, L. K.; Compton, L. D.; Miller, L. L.; Baker, D. S.; Pesheck, C. V.; Lord,

R. S. Pharmacokinetics, metabolism, and excretion of irinotecan (CPT-11) following i.v. infusion of [^{14}C]CPT-11 in cancer patients. *Drug Metab. Dispos.* **2000**, *28*, 423–433.

(50) Antony, S.; Agama, K. K.; Miao, Z.-H.; Takagi, K.; Wright, M. H.; Robles, A. I.; Varticovski, L.; Nagarajan, M.; Morrell, A.; Cushman, M.; Pommier, Y. Novel indenoisoquinolines NSC 725776 and NSC 724998 produce persistent topoisomerase I cleavage complexes and overcome multidrug resistance. *Cancer Res.* **2007**, *67*, 10397–10405.

(51) Das, S. K.; Rehman, I.; Ghosh, A.; Sengupta, S.; Majumdar, P.; Jana, B.; Das, B. B. Poly(ADP-ribose) polymers regulate DNA topoisomerase I (top1) nuclear dynamics and camptothecin sensitivity in living cells. *Nucleic Acids Res.* **2016**, *44*, 8363–8375.

(52) Rehman, I.; Basu, S. M.; Das, S. K.; Bhattacharjee, S.; Ghosh, A.; Pommier, Y.; Das, B. B. PRMT5-mediated arginine methylation of TDP1 for the repair of topoisomerase I covalent complexes. *Nucleic Acids Res.* **2018**, *46*, 5601–5617.

(53) Das, B. B.; Huang, S.-y. N.; Murai, J.; Rehman, I.; Amé, J.-C.; Sengupta, S.; Das, S. K.; Majumdar, P.; Zhang, H.; Biard, D.; Majumder, H. K.; Schreiber, V.; Pommier, Y. PARP1-TDP1 coupling for the repair of topoisomerase I-induced DNA damage. *Nucleic Acids Res.* **2014**, *42*, 4435–4449.

(54) Das, B. B.; Antony, S.; Gupta, S.; Dexheimer, T. S.; Redon, C. E.; Garfield, S.; Shiloh, Y.; Pommier, Y. Optimal function of the DNA repair enzyme TDP1 requires its phosphorylation by ATM and/or DNA-PK. *EMBO J.* **2009**, *28*, 3667–3680.

(55) Furuta, T.; Takemura, H.; Liao, Z.-Y.; Aune, G. J.; Redon, C.; Sedelnikova, O. A.; Pilch, D. R.; Rogakou, E. P.; Celeste, A.; Chen, H. T.; Nussenzweig, A.; Aladjem, M. I.; Bonner, W. M.; Pommier, Y. Phosphorylation of histone H2AX and activation of Mre11, Rad50, and Nbs1 in response to replication-dependent DNA double-strand breaks induced by mammalian DNA topoisomerase I cleavage complexes. *J. Biol. Chem.* **2003**, *278*, 20303–20312.

(56) Sordet, O.; Redon, C. E.; Guirouilh-Barbat, J.; Smith, S.; Solier, S.; Douarre, C.; Conti, C.; Nakamura, A. J.; Das, B. B.; Nicolas, E.; Kohn, K. W.; Bonner, W. M.; Pommier, Y. Ataxia telangiectasia mutated activation by transcription- and topoisomerase I-induced DNA double-strand breaks. *EMBO Rep.* **2009**, *10*, 887–893.

(57) Pommier, Y.; Sun, Y.; Huang, S.-y. N.; Nitiss, J. L. Roles of eukaryotic topoisomerases in transcription, replication and genomic stability. *Nat. Rev. Mol. Cell Biol.* **2016**, *17*, 703–721.

(58) Covey, J. M.; Jaxel, C.; Kohn, K. W.; Pommier, Y. Protein-linked DNA strand breaks induced in mammalian cells by camptothecin, an inhibitor of topoisomerase I. *Cancer Res.* **1989**, *49*, 5016–5022.

(59) Ashour, M. E.; Atteya, R.; El-Khamisy, S. F. Topoisomerase-mediated chromosomal break repair: an emerging player in many games. *Nat. Rev. Cancer* **2015**, *15*, 137–151.

(60) Das, B. B.; Dexheimer, T. S.; Maddali, K.; Pommier, Y. Role of tyrosyl-DNA phosphodiesterase (TDP1) in mitochondria. *Proc. Natl. Acad. Sci. U.S.A.* **2010**, *107*, 19790–19795.